

Resummation of $\tan \beta$ -enhanced supersymmetric loop corrections beyond the decoupling limit

Lars Hofer, Ulrich Nierste and Dominik Scherer

*Institut für Theoretische Teilchenphysik
Karlsruhe Institute of Technology, Universität Karlsruhe
D-76128 Karlsruhe, Germany*

Abstract

We study the Minimal Supersymmetric Standard Model with Minimal Flavour Violation for the case of a large parameter $\tan \beta$ and arbitrary values of the supersymmetric mass parameters. We derive several resummation formulae for $\tan \beta$ -enhanced loop corrections, which were previously only known in the limit of supersymmetric masses far above the electroweak scale. Studying first the renormalisation-scheme dependence of the resummation formula for the bottom Yukawa coupling, we clarify the use of the sbottom mixing angle in the supersymmetric loop factor Δ_b . As a new feature, we find $\tan \beta$ -enhanced loop-induced flavour-changing neutral current (FCNC) couplings of gluinos and neutralinos which in turn give rise to new effects in the renormalisation of the Cabibbo-Kobayashi-Maskawa matrix and in FCNC processes of B mesons. For the chromomagnetic Wilson coefficient C_8 , these gluino-squark loops can be of the same size as the known chargino-squark contribution. We discuss the phenomenological consequences for the mixing-induced CP asymmetry in $B_d \rightarrow \phi K_S$. We further quote formulae for $B_s \rightarrow \mu^+ \mu^-$ and $B_s - \bar{B}_s$ mixing valid beyond the decoupling limit and find a new contribution affecting the phase of the $B_s - \bar{B}_s$ mixing amplitude. Our resummed $\tan \beta$ -enhanced effects are cast into Feynman rules permitting an easy implementation in automatic calculations.

Contents

1	Introduction	2
2	Diagrammatic resummation: the flavour-conserving case	7
2.1	The method	7
2.2	Sbottom mixing and resummation	11
3	Flavour mixing at large $\tan \beta$	13
3.1	Flavour-changing self-energies in external legs	15
3.2	Renormalisation of the flavour-changing self-energies	17
3.3	Formulation of Feynman rules for the large- $\tan \beta$ scenario	20

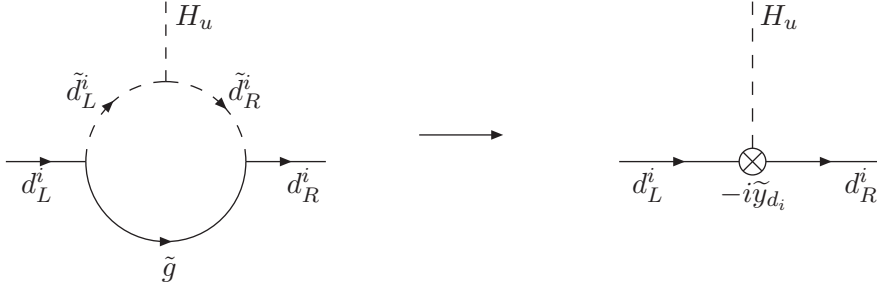
4 Phenomenology: FCNC processes	22
4.1 The effective $ \Delta B = 1$ Hamiltonian	23
4.2 The effective $ \Delta B = 2$ Hamiltonian	27
5 Numerical study of $C_{7,\tilde{g}}$ and $C_{8,\tilde{g}}$ and implications for $\bar{B}^0 \rightarrow \phi K_S$	29
6 Conclusions	32
A Conventions	34
A.1 Squark mixing	34
A.2 Chargino mixing	36
A.3 Loop functions	37
B QCD corrections to flavour-changing self-energies	37
C Feynman rules	39

1 Introduction

The Minimal Supersymmetric Standard Model (MSSM) contains two Higgs doublets H_u and H_d , whose Yukawa couplings to quarks are given by

$$\mathcal{L}_y = -y_u^{ij} \bar{u}_R^i Q_j^T \epsilon H_u + y_d^{ij} \bar{d}_R^i Q_j^T \epsilon H_d + \text{h.c.} \quad (1)$$

Here Q_j , u_R^i and d_R^i are the usual left-handed doublet and right-handed singlet quark fields, ϵ is the antisymmetric 2×2 matrix with $\epsilon_{12} = -\epsilon_{21} = 1$, and y_u and y_d are Yukawa matrices with generation indices $i, j = 1, 2, 3$. The holomorphy of the superpotential forbids couplings of H_u to d_R and of H_d to u_R , so that the Yukawa Lagrangian of Eq. (1) is that of a two-Higgs-doublet model (2HDM) of type II. The neutral components of the Higgs doublets acquire vacuum expectation values (vevs) v_u and v_d with $v = \sqrt{v_u^2 + v_d^2} \approx 174$ GeV leading to quark mass matrices $M_u = y_u v_u$ and $M_d = y_d v_d$. Unitary rotations of the quark fields in flavour space diagonalise these matrices, the resulting basis of mass eigenstates is no more a weak basis (with manifest SU(2) symmetry) and the familiar Cabibbo-Kobayashi-Maskawa (CKM) matrix appears in the couplings of the W boson to the quark fields. As long as only the tree-level couplings of \mathcal{L}_y are considered the Yukawa couplings are diagonal in flavour space, $y_q^{ij} = y_{qj} \delta_{ij}$ (no sum over j). At this point no flavour-changing couplings of neutral Higgs bosons occur and the diagonal Yukawa couplings are easily expressed in terms of quark masses m_{qj} and $\tan \beta \equiv v_u/v_d$: $y_{d_j} = m_{d_j}/v_d = m_{d_j}/(v \cos \beta)$ and $y_{u_j} = m_{u_j}/v_u = m_{u_j}/(v \sin \beta)$. If $\tan \beta$ is large, the Higgs couplings to down-type fermions can be enhanced to a level which is detectable in present-day B physics experiments. In particular, for $\tan \beta = \mathcal{O}(50)$ the bottom Yukawa coupling $y_b = y_{d_3}$ can be of order 1. A theoretical motivation of such large values of $\tan \beta$ is given by bottom-top Yukawa unification, which occurs in SO(10) GUT models with minimal Yukawa sector.

Figure 1: Effective coupling of the down-type quarks to H_u

Phenomenologically, the anomalous magnetic moment of the muon invites large values of $\tan \beta$ [1], but the current situation is inconclusive in the light of recent experimental data on the hadroproduction cross section measured by BaBar [2].

Once soft supersymmetry-breaking terms are considered, the pattern described above changes dramatically: As pointed out first by Banks, one-loop diagrams induce an effective coupling of H_u to d_R^j [3]. Hall, Rattazzi and Sarid then discovered the relevance of this loop contribution for large- $\tan \beta$ phenomenology [4–6]. If M_{SUSY} , the mass scale of the supersymmetry-breaking terms, is much larger than the masses and vevs of the Higgs sector, we can integrate out the SUSY particles. The resulting effective Lagrangian is that of a general 2HDM, different from the type-II 2HDM which we encounter at tree-level. In the Super-CKM basis for the quark and squark fields, in which $y_d^{ij} = y_{d_i} \delta^{ij}$, the Yukawa couplings of down-type quarks are given by the effective Lagrangian

$$\mathcal{L}_{y,d}^{\text{eff}} = y_{d_i} \bar{d}_R^i Q_i^T \epsilon H_d - \tilde{y}_d^{ij} \bar{d}_R^i Q_j^T H_u^* + \text{h.c.} \quad (2)$$

In this paper we restrict ourselves to the case that the soft SUSY-breaking terms are flavour-diagonal in the Super-CKM basis. As a consequence, all gluino-squark-quark and neutralino-squark-quark couplings in the MSSM Lagrangian are flavour-diagonal. Further the chargino-squark-quark couplings come with the same CKM elements as the corresponding couplings of W bosons or charged Higgs bosons to (s)quarks. This scenario of naive Minimal Flavour Violation (naive MFV) occurs if e.g. supersymmetry is broken at a low scale by a flavour-blind mechanism leading to flavour-universal squark mass matrices. (A symmetry-based and RG-invariant definition of MFV has been proposed in [7]. For a recent analysis see Ref. [8].) In our version of naive MFV, however, we slightly go beyond flavour universality, as we allow the SUSY-breaking terms of the third generation to be different from those of the first two generations. In this way we also include the cases of the widely-studied CMSSM (see e.g. Refs. [9, 10] for recent studies) and mSUGRA [11–16] models, in which renormalisation-group (RG) effects involving the large top and bottom Yukawa couplings destroy the universal boundary condition imposed at the GUT scale. In such models with high-scale flavour universality the RG also induces flavour-violating gluino and neutralino couplings at the electroweak scale, but their impact on FCNC transitions like $B - \bar{B}$ mixing and $b \rightarrow s \gamma$ is small [17, 18] and the naive MFV pattern essentially stays intact. On the other hand, the universality of the flavour-diagonal SUSY-breaking terms is badly broken at low energies, e.g. the trilinear term of the third generation A_t substantially differs from $A_u \simeq A_c$. We emphasize that no variant of the MFV assumption forbids flavour-diagonal CP-violating phases [19]. Such phases appear in A_t , the higgsino mass parameter μ , and the gaugino mass terms M_i , $i = 1, 2, 3$, which we consequently always treat as complex quantities throughout our analysis.

The dominant contribution to the effective coupling \tilde{y}_d^{ij} stems from a gluino-squark loop and is de-

picted in Fig. 1. In naive MFV, the corresponding contribution to \tilde{y}_d^{ij} is $\tilde{y}_{d_i}^{\tilde{g}} \delta_{ij}$ with

$$\begin{aligned} \tilde{y}_{d_i}^{\tilde{g}} &= y_{d_i} \cdot \epsilon_i^{\tilde{g}}(\mu, m_{\tilde{d}_L^i}, m_{\tilde{d}_R^i}), \\ \text{and} \quad \epsilon_i^{\tilde{g}}(\mu, m_{\tilde{d}_L^i}, m_{\tilde{d}_R^i}) &= -\frac{2\alpha_s}{3\pi} m_{\tilde{g}} \mu^* C_0(m_{\tilde{g}}, m_{\tilde{d}_L^i}, m_{\tilde{d}_R^i}). \end{aligned} \quad (3)$$

Here $m_{\tilde{d}_L^i}^2$ and $m_{\tilde{d}_R^i}^2$ are the mass terms for the left-handed and right-handed down-squarks of the i -th generation, respectively, $m_{\tilde{g}}$ is the gluino mass and the loop integral C_0 is defined in Appendix A. Accounting for similar contributions from loops with charginos (still neglecting flavour mixing) or neutralinos we write $\epsilon_i = \epsilon_i^{\tilde{g}} + \epsilon_i^{\tilde{\chi}^\pm} + \epsilon_i^{\tilde{\chi}^0}$. Both terms in $\mathcal{L}_{y,d}^{\text{eff}}$ of Eq. (2) contribute to the masses of down-type quarks. The ratio of the two contributions is

$$\Delta_i \equiv \frac{\tilde{y}_{d_i} v_u}{y_{d_i} v_d} = \epsilon_i \cdot \tan \beta. \quad (4)$$

A large value of $\tan \beta$ can compensate for the loop factor ϵ_i rendering $\Delta_i = \mathcal{O}(1)$. The relation between the Yukawa coupling y_{d_i} and the physical quark mass m_{d_i} is therefore modified substantially:

$$y_{d_i} = \frac{m_{d_i}}{v_d(1 + \Delta_i)}. \quad (5)$$

Several papers have studied the impact of Δ_i on Yukawa unification [4, 6], neutral [20] and charged Higgs [21] phenomenology.

Later Hamzaoui, Pospelov and Toharia have discovered that \tilde{y}_d^{ij} has a profound impact on flavour physics: The down-quark mass matrix M_d computed from $\mathcal{L}_{y,d}^{\text{eff}}$ will be non-diagonal and conversely a non-diagonal Yukawa coupling y_d^{ij} appears in the basis of mass eigenstates [22]. The resulting FCNC couplings of the non-standard neutral Higgs bosons H^0 and A^0 are loop-suppressed but involve two powers of $\tan \beta$. Thus the new FCNC couplings may compete in size with the flavour-diagonal tree-level coupling which involves a single power of $\tan \beta$ and is of order 1 in the case of the bottom quark. Importantly, these effects are already highly relevant in naive MFV, where only chargino-loops contribute to the off-diagonal entries of \tilde{y}_d^{ij} , which moreover involve the same small CKM elements as the SM contribution. In our effective theory, the general 2HDM with $\mathcal{L}_{y,d}^{\text{eff}}$ in Eq. (2), FCNC processes proceed through tree diagrams with H^0 or A^0 exchange. Most spectacular effects occur in $B_{d,s} \rightarrow \ell^+ \ell^-$ decays, where a priori orders-of-magnitude effects were possible even in the MSSM with naive MFV [23]. The dominant Higgs-mediated contribution to $\mathcal{B}(B_{d,s} \rightarrow \ell^+ \ell^-)$ is proportional to six powers of $\tan \beta$ and $\mathcal{B}(B_{d,s} \rightarrow \ell^+ \ell^-)$ is more sensitive to the large- $\tan \beta$ region of the MSSM than any other decay rate or cross section. A correlated analysis of $\mathcal{B}(B_{d,s} \rightarrow \ell^+ \ell^-)$ with the muon anomalous magnetic moment has been performed in Ref. [24]. The presence of \tilde{y}_d^{ij} in $\mathcal{L}_{y,d}^{\text{eff}}$ further leads to a modification of the relation between y_d^{ij} and the CKM elements by $\tan \beta$ -enhanced loop corrections. This feature was studied in Ref. [25] in MFV well before the discovery of the Higgs-mediated FCNC effects.¹ As a consequence, the couplings of the charged Higgs boson to down-type fermions are modified, with phenomenological impact on $B^+ \rightarrow \tau^+ \nu$ [27] and $B^+ \rightarrow D \tau^+ \nu$ [28, 29].

$B - \bar{B}$ mixing plays a special role: The superficially leading contribution from diagrams with right-handed b -quark fields vanishes [22], because the two diagrams with H^0 and A^0 exchange cancel each other. Buras et al. have discovered that, despite of a suppression factor of m_s/m_b , the analogous diagrams with one right-handed s -quark field can sizably diminish $B_s - \bar{B}_s$ mixing [30]. This effect is

¹Recently, this finite CKM renormalisation has been extended to the case of non-minimal flavour violation [26].

highly correlated with $\mathcal{B}(B_s \rightarrow \ell^+ \ell^-)$ and today's upper bound on $\mathcal{B}(B_s \rightarrow \mu^+ \mu^-)$ from the Tevatron experiments [31, 32] severely limits the size of the Higgs-mediated contribution in $B_s - \bar{B}_s$ mixing [33]. In subsequent papers further contributions such as the charged-Higgs box diagram to $B - \bar{B}$ mixing [34] and contributions to \tilde{y}_d^{ij} involving the electroweak gauge couplings were considered [35, 36]. A complete list of all one-loop contributions to \tilde{y}_d^{ij} for the case of universal SUSY-breaking terms taking into account all possible CP phases can be found in Ref. [36]. The absence of the superficially dominant contribution renders $B - \bar{B}$ mixing vulnerable to other subleading corrections proportional to other small expansion parameters such as $\cot \beta$, v/M_{SUSY} or the loop factor $1/(16\pi^2)$. Any of these corrections could potentially spoil the cancellation and endanger the correlation found in [30]. The recent symmetry-based analysis of Ref. [36] has revealed that all these subleading corrections are small and the correlation found in Ref. [33] essentially stays intact. An important ingredient of this study are contributions to $B - \bar{B}$ mixing stemming from loop corrections to the Higgs potential. At this point the appropriate definition of $\tan \beta$, which is ill-defined in a general 2HDM, had to be clarified. Loop corrections to $B - \bar{B}$ mixing from the Higgs potential were also calculated in Ref. [37]. In view of the findings of Refs. [36, 37] we neglect all radiative contributions to Higgs self-couplings and work with the tree-level Higgs potential of the MSSM. The latter is CP-conserving; we can work with the usual Higgs mass eigenstates with definite CP quantum numbers (i.e. the CP-odd A^0 and the CP-even h^0, H^0) and all CP-violation discussed in this paper enters through the (loop-corrected) Yukawa sector.

The last three paragraphs have addressed Higgs couplings to right-handed down-type quarks which involve a factor of $\tan \beta$ at tree-level. A different type of $\tan \beta$ -enhanced corrections occurs in Higgs couplings of the right-handed top-quark field, which are suppressed by a factor of $\cot \beta$ at tree level. A prominent example is the $\bar{t}_{RL} H^+$ coupling entering the charged-Higgs loop in $b \rightarrow s \gamma$. Supersymmetric vertex corrections lift the $\cot \beta$ suppression and the one-loop correction competes with the tree-level coupling [38, 39]. In the decoupling limit also these effects can be easily described by an effective Lagrangian $\mathcal{L}_{y,u}^{\text{eff}}$, which in addition to the first term in Eq. (1) contains an effective loop-induced coupling \tilde{y}_u^{ij} involving H_u^* .

The appearance of the $\tan \beta$ -enhanced supersymmetric loop correction Δ_i in the denominator of y_i in Eq. (5) signals the resummation of this correction to all orders in perturbation theory. As a drawback, the effective-field-theory method is only valid for $M_{\text{SUSY}} \gg v, M_{A^0}, M_{H^0}, M_{H^\pm}$. This is unsatisfactory, since in supersymmetry one naturally expects $M_{\text{SUSY}} \sim v$, especially if the electroweak symmetry is broken radiatively. One needs an unnatural fine-tuning in the Higgs potential to achieve $M_{\text{SUSY}} \gg M_{A^0}, M_{H^0}, M_{H^\pm}$ [37]. After all the widely-studied scenarios with neutralino LSP involve several supersymmetric particles with masses around and below v . Of course, several authors have discovered $\tan \beta$ -enhanced loop corrections within diagrammatical one-loop calculations in the MSSM [40, 41]. Yet only four papers have studied $\tan \beta$ -enhanced corrections with their subsequent resummation beyond the $M_{\text{SUSY}} \gg v$ limit: In Ref. [21] the $\tan \beta$ -enhanced diagrams contributing to Δ_i have been identified to all orders and have been explicitly resummed. The result of Ref. [21] mimics the form of Eq. (5), but Δ_i involves squark mass eigenstates and its validity does not assume any hierarchy between v and M_{SUSY} . In Ref. [42] the method of Ref. [21] has been applied to the lepton sector in an analysis of the muon anomalous magnetic moment. The authors of Ref. [35] have calculated Higgs-mediated FCNC processes to one-loop order for arbitrary M_{SUSY} , but relied on the effective-field-theory formalism for the all-order resummation. In Ref. [19] the $\tan \beta$ -enhanced corrections to the Yukawa sector have been incorporated in an effective-potential approach, with a proper consideration of all CP phases of the MSSM. The results of Refs. [19, 35] permit the resummation of the flavour-changing $\tan \beta$ -enhanced corrections through an iterative procedure, which converges

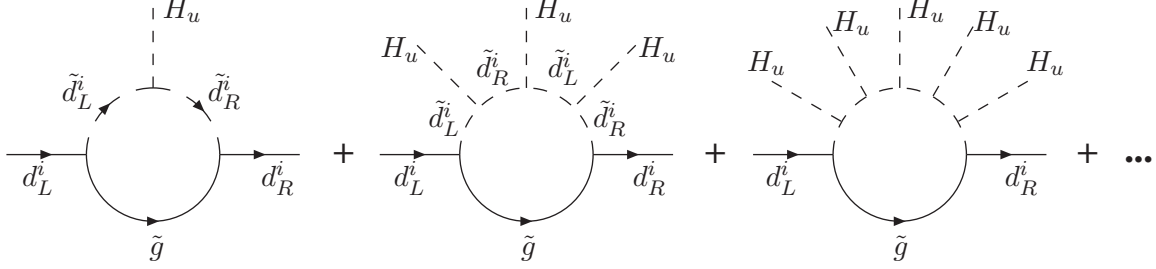


Figure 2: Series of ‘hedgehog diagrams’ contributing to m_{d_i}

if the magnitude of these resummed corrections are numerically smaller than 1. We present analytical resummation formulae in this paper corresponding to the limits to which the iterative method converges.

It is illustrative to consider the extension of the effective-field-theory formalism to subleading powers in v^2/M_{SUSY}^2 : To this end we must add higher-dimensional couplings to $\mathcal{L}_y^{\text{eff}}$ involving more H_u fields. The gluino contributions to these new effective couplings are shown in Fig. 2. Interestingly, in this simple case one can sum the contributions of these ‘hedgehog diagrams’ to m_{d_i} to all orders in v^2/M_{SUSY}^2 : The result has again the form of Eq. (5) with $\epsilon_i^{\tilde{g}}$ of Eq. (4) replaced as

$$\epsilon_i^{\tilde{g}}(\mu, m_{\tilde{d}_L^i}, m_{\tilde{d}_R^i}) \rightarrow \epsilon_i^{\tilde{g}}(\mu, m_{\tilde{d}_1^i}, m_{\tilde{d}_2^i}), \quad (6)$$

where $m_{\tilde{d}_{1,2}^i}$ denote the physical squark masses, i.e. the eigenvalues of the squark mass matrix. Using this expression in Eqs. (4) and (5) reproduces the result of the diagrammatic resummation of Ref. [21]. The information encoded in the diagrams of Fig. 2 is also contained in the one-loop effective functional of Ref. [19].

In this paper we derive formulae for the resummation of $\tan\beta$ -enhanced corrections which are valid for any value of M_{SUSY} . As in any analysis of radiative corrections this requires the full control over the renormalisation scheme of the parameters in the MSSM Lagrangian. This can be achieved with the diagrammatic method of Ref. [21], but is very difficult to achieve with the effective-field-theory formalism, even if one succeeds to resum the series in v^2/M_{SUSY}^2 as in Eq. (6). The origin of this difficulty is readily understood: While resummation formulae derived from $\mathcal{L}_y^{\text{eff}}$ correspond to a decoupling scheme for the MSSM parameters, any two of such schemes may differ by terms of order v/M_{SUSY} and the corresponding resummation formulae look different. The plan of the paper is as follows: In Sect. 2 we first recall the diagrammatic resummation method and then address the open issues of the case without flavour mixing. In particular we clarify the renormalisation scheme of the sbottom mixing angle and derive analytic expressions for $\Delta_b \equiv \Delta_3$ for three different schemes. In Sect. 3 we resum the $\tan\beta$ -enhanced loop effects in FCNC processes. Sect. 4 is devoted to an analysis of $\tan\beta$ -enhanced corrections to FCNC processes in B physics. Sect 5 contains a numerical study of the Wilson coefficients C_7 and C_8 and an analysis of novel effects in $B \rightarrow \phi K_S$. Finally we conclude.

2 Diagrammatic resummation: the flavour-conserving case

We use the conventions of the SUSY Les Houches Accord (SLHA) [43] for the MSSM parameters. Several of these parameters carry complex phases, but only certain phase differences are physical, CP-violating quantities. We choose a phase convention in which the gluino mass parameter M_3 is real and positive, so that $M_3 = m_{\tilde{g}}$. The phases entering the left-right mixing of squarks are unspecified by the SLHA and are defined in Appendix A, where also our conventions for the loop integrals can be found. We always work in the Super-CKM basis, in which the Yukawa matrices are diagonal in flavour space. For definiteness we consider the quark sector only and in our discussion of flavour-diagonal effects we usually quote the results for the b quark. The expressions generalise to the case of the τ lepton in a straightforward way, by dropping the gluino contributions, replacing squarks by sleptons and changing the hypercharges in the couplings appropriately.

2.1 The method

There are two potential sources of $\tan \beta$ -enhanced corrections,

- i) the (renormalised) MSSM Lagrangian \mathcal{L} and
- ii) the transition matrix element \mathcal{M} from which the process of interest is calculated.

We first identify the enhanced corrections at one-loop order and turn to higher orders (and the resummation) afterwards. To address point i) we decompose \mathcal{L} in the usual way as $\mathcal{L} = \mathcal{L}_{\text{ren}} + \mathcal{L}_{\text{ct}}$, where \mathcal{L}_{ren} is obtained from \mathcal{L} by replacing bare quantities by renormalised ones and \mathcal{L}_{ct} contains the counterterms. Loop effects only reside in \mathcal{L}_{ct} and the quark mass counterterm δm_b is a source of $\tan \beta$ -enhanced corrections. We write m_b for the renormalised mass, so that the bare mass reads $m_b^{(0)} = m_b + \delta m_b$. The mass term in \mathcal{L} is

$$\mathcal{L}_m = - m_b^{(0)} \bar{b}_R b_L - m_b^{(0)*} \bar{b}_L b_R = - m_b \bar{b} b - \delta m_b \bar{b}_R b_L - \delta m_b^* \bar{b}_L b_R. \quad (7)$$

Here we have taken into account that δm_b must be complex to render m_b real if the loops canceled by δm_b involve complex parameters. We further decompose the self-energy $\Sigma_b(p)$ as

$$\Sigma_b(p) = \not{p} [\Sigma_b^{LL}(p^2) P_L + \Sigma_b^{RR}(p^2) P_R] + \Sigma_b^{RL}(p^2) P_L + \Sigma_b^{LR}(p^2) P_R \quad (8)$$

with $\Sigma_b^{LR}(p^2) = (\Sigma_b^{RL}(p^2))^*$,

where $P_{L,R} = (1 \mp \gamma_5)/2$ and p is the external momentum. If the mass is renormalised on-shell, i.e. if m_b coincides with the pole of the propagator, the counterterm reads

$$\delta m_b = -\frac{m_b}{2} [\Sigma_b^{LL}(m_b^2) + \Sigma_b^{RR}(m_b^2)] - \Sigma_b^{RL}(m_b^2). \quad (9)$$

The second term $\Sigma_b^{RL}(m_b^2)$ contains pieces proportional to $y_b v \sin \beta$ and is therefore $\tan \beta$ -enhanced compared to the tree-level term $m_b = y_b v \cos \beta$. These contributions are depicted in Fig. 3 and read:

$$\Sigma_b^{RL} = m_b \Delta_b \quad \text{with} \quad \Delta_b = \Delta_b^{\tilde{g}} + \Delta_b^{\tilde{\chi}^\pm} + \Delta_b^{\tilde{\chi}^0} \quad (10)$$

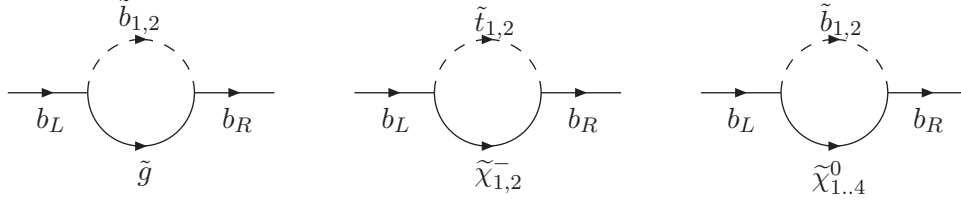


Figure 3: $\tan \beta$ -enhanced self-energy diagrams with (from left to right) gluinos, charginos and neutralinos.

and

$$\Delta_b^{\tilde{g}} = \frac{\alpha_s m_{\tilde{g}}}{3\pi m_b} \sin 2\tilde{\theta}_b e^{-i\tilde{\phi}_b} \cdot \left[B_0(m_{\tilde{g}}, m_{\tilde{b}_1}) - B_0(m_{\tilde{g}}, m_{\tilde{b}_2}) \right], \quad (11)$$

$$\Delta_b^{\tilde{\chi}^\pm} = -\frac{g^2}{16\pi^2 \cos \beta} \sum_{m=1}^2 \left\{ \frac{m_{\tilde{\chi}_m^\pm}}{2\sqrt{2}M_W} \frac{y_t}{g} \tilde{U}_{m2}^* \tilde{V}_{m2}^* \sin 2\tilde{\theta}_t e^{i\tilde{\phi}_t} \cdot \left[B_0(m_{\tilde{\chi}_m^\pm}, m_{\tilde{t}_1}) - B_0(m_{\tilde{\chi}_m^\pm}, m_{\tilde{t}_2}) \right] \right. \\ \left. - \frac{m_{\tilde{\chi}_m^\pm}}{\sqrt{2}M_W} \tilde{U}_{m2}^* \tilde{V}_{m1}^* \left[\cos^2 \tilde{\theta}_t B_0(m_{\tilde{\chi}_m^\pm}, m_{\tilde{t}_1}) + \sin^2 \tilde{\theta}_t B_0(m_{\tilde{\chi}_m^\pm}, m_{\tilde{t}_2}) \right] \right\}, \quad (12)$$

$$\Delta_b^{\tilde{\chi}^0} = \frac{g^2}{16\pi^2 \cos \beta} \sum_{m=1}^4 \frac{m_{\tilde{\chi}_m^0}}{2M_W} \tilde{N}_{m2}^* \tilde{N}_{m3}^* \cdot \left[\cos^2 \tilde{\theta}_b B_0(m_{\tilde{\chi}_m^0}, m_{\tilde{b}_1}) + \sin^2 \tilde{\theta}_b B_0(m_{\tilde{\chi}_m^0}, m_{\tilde{b}_2}) \right]. \quad (13)$$

In (13) we have neglected some numerically small contributions: First, a term proportional to g'^2 stemming from the bino component of the neutralinos is omitted. Second, a numerically small term proportional to g^2 (which moreover is suppressed by $(v/M_{\text{SUSY}})^2$ for large M_{SUSY} and is therefore absent in the effective Lagrangian of Eq. (2)) is neglected. Clearly, we have also discarded terms suppressed by m_b^2/M_{SUSY}^2 ; in particular Σ_b^{RL} is evaluated for $p^2 = 0$. Whereas in the effective-theory approach the $\tan \beta$ -enhancement was easily recognisable by the coupling to H_u , in the diagrammatic treatment it is hidden in the elements of the mixing matrices. Using the analytic expressions for these matrices listed in Appendix A, i.e. identities like Eq. (109) and Eqs. (118–121), we can derive formulae for the gluino- and chargino-contributions in which the $\tan \beta$ -enhancement becomes explicit. Writing

$$\Delta_b^K = \epsilon_b^K \tan \beta \quad \text{for } K = \tilde{g}, \tilde{\chi}^\pm, \tilde{\chi}^0 \quad \text{and} \quad \epsilon_b = \epsilon_b^{\tilde{g}} + \epsilon_b^{\tilde{\chi}^\pm} + \epsilon_b^{\tilde{\chi}^0} \quad (14)$$

we find

$$\epsilon_b^{\tilde{g}} = -\frac{2\alpha_s}{3\pi} m_{\tilde{g}} \mu^* C_0(m_{\tilde{g}}, m_{\tilde{b}_1}, m_{\tilde{b}_2}), \quad (15)$$

$$\epsilon_b^{\tilde{\chi}^\pm} = -\frac{y_t^2}{16\pi^2} A_t^* \mu^* (D_2 - |M_2|^2 D_0) + \frac{g^2}{16\pi^2} \mu^* M_2^* (D_2 - m_{\tilde{t}_R}^2 D_0), \quad (16)$$

where $D_{0,2} = D_{0,2}(m_{\tilde{\chi}_1^\pm}, m_{\tilde{\chi}_2^\pm}, m_{\tilde{t}_1}, m_{\tilde{t}_2})$. (The $\tan \beta$ -enhancement of $\Delta_b^{\tilde{\chi}^0}$ is already manifest in Eq. (13) through the factor $1/\cos \beta \simeq \tan \beta$.) Formulae analogous to Eqs. (11–16) are also valid for the corresponding self-energies of the d- and the s-quark with the stop and sbottom masses appropriately replaced by the corresponding squark masses of the first or second generation. Eqs. (11–16) generalise the well-known expressions of Ref. [44] to the case of complex MSSM parameters.

Different renormalisation schemes correspond to different choices of \mathcal{L}_{ct} , hence the analytic form of the $\tan \beta$ -enhanced corrections depends on the chosen scheme. If we want to use a numerical value for m_b determined from low-energy data, we must apply an on-shell subtraction to the supersymmetric loops as in Eq. (9) (which is the appropriate “decoupling scheme”). To leading order in $\tan \beta$ this means

$$\delta m_b = -\Sigma_b^{RL} = -m_b \epsilon_b \tan \beta. \quad (17)$$

At this point we recall that the loops constituting ϵ_b are finite, just as all other $\tan \beta$ -enhanced loops appearing in this paper. Therefore all counterterms and all bare quantities discussed are finite as well. We write the bare Yukawa couplings as $y_b^{(0)} = y_b + \delta y_b$, where y_b is the renormalised coupling and δy_b is the counterterm. The choice of δm_b fixes δy_b through

$$\delta y_b = \frac{\delta m_b}{v_d} = -y_b \epsilon_b \tan \beta. \quad (18)$$

The supersymmetric loop effects encoded in ϵ_b enter physical observables only through δy_b . Choosing e.g. a minimal subtraction for δm_b would remove the $\tan \beta$ -enhanced term from Eq. (18) and there would be nothing to resum. However, in this scheme the input value for m_b is obtained from the measured bottom mass by adding $m_b \epsilon_b \tan \beta$. Thus the inferred value of $y_b = m_b/v_d$ will implicitly contain the $\tan \beta$ -enhanced corrections, so that physical observables are scheme-independent [21]. In a practical application one must also address the renormalisation from ordinary QCD corrections. Whenever we refer to the $\overline{\text{MS}}$ mass m_b we imply that the $\overline{\text{MS}}$ prescription is applied to the quark-gluon loop only, while we always subtract the supersymmetric loops on-shell.

Now, are there other sources of $\tan \beta$ -enhanced one-loop corrections in \mathcal{L}_{ct} ? There are renormalisation schemes proposed in the literature in which the counterterm to $\tan \beta$ is proportional to $\tan^2 \beta$, so that Eq. (18) would receive an additional contribution. This feature is obviously absent for the commonly used definition of $\tan \beta$ in the $\overline{\text{DR}}$ scheme. Finally the one-loop renormalisation also involves wave-function counterterms. Those of the quark fields are not $\tan \beta$ -enhanced and the wave-function counterterms of the Higgs fields drop out if the Higgses solely occur in internal lines of the diagrams. (These counterterms nevertheless play a role in schemes in which the counterterm $\delta \tan \beta$ is derived from wave-function counterterms and counterterms to the vevs. This subtlety is absent for the $\overline{\text{DR}}$ -defined $\delta \tan \beta$.) The issue of $\tan \beta$ renormalisation is thoroughly analysed in Refs. [45–47] and was recently studied for quark flavour physics in the context of the effective-field-theory method [36, 37]. In our diagrammatic approach, where the issue is somewhat simpler, the topic of $\tan \beta$ renormalisation is briefly discussed in Ref. [42] in an application to the muon anomalous magnetic moment. In conclusion, the only source of $\tan \beta$ -enhanced corrections in \mathcal{L}_{ct} is δy_b of Eq. (18) unless an inappropriate definition of $\tan \beta$ is adopted.

Next we turn to the second point mentioned at the beginning of this section. In order to identify $\tan \beta$ -enhanced corrections to a given transition matrix element \mathcal{M} we must distinguish two cases: In the first case the leading-order contribution to \mathcal{M} has no suppression factor of $\cot \beta$ in any coupling. Examples for such unsuppressed couplings are those of A^0 and H^0 to down-type quarks, the H^+ coupling to right-handed down-type quarks or any gauge coupling. In this situation \mathcal{M} can only have a $\tan \beta$ -enhanced correction if the loop integral involves at least one inverse power of m_b , which combines with $y_b \propto m_b \tan \beta$ to a factor of $\tan \beta$. The presence of such inverse powers of m_b is related to the infrared behaviour of \mathcal{M} for $m_b \rightarrow 0$. This behaviour can be studied by matching \mathcal{M} onto an effective matrix element \mathcal{M}_{eff} which is obtained from \mathcal{M} by contracting all lines of particles heavier than m_b to a point [21]. This analysis should not be confused with the effective-field-theory method described in the Introduction: Here only $M_{\text{SUSY}}, v, M_{A^0}, M_{H^0}, M_{H^\pm} \gg m_b$ is assumed,

with no assumption on the hierarchy between M_{SUSY} and v . The result of Ref. [21] is that no such $\tan \beta$ -enhanced correction from genuine multi-loop diagrams occur in the first case. The second case deals with matrix elements \mathcal{M} with an explicit $\cot \beta$ -suppressed coupling (such as the h^0 coupling to down-type quarks or the H^+ coupling to left-handed down-type quarks) in the leading order. Here the situation is different, but trivial: An explicit one-loop vertex correction lifts the suppression and this $\tan \beta$ -enhanced correction does not replicate itself in higher orders [38, 39].

We now discuss higher orders of the perturbative expansion and the resummation: While no genuine multi-loop diagrams give enhanced corrections, there are one-loop diagrams involving lower-order counterterms δy_b . We make the y_b -dependence of the self-energy explicit by writing $\Sigma_b^{RL}(y_b)$. The Yukawa coupling y_b enters $\Sigma_b^{RL}(y_b)$ either directly via the quark-squark-higgsino-vertex or indirectly via the sbottom mixing angle. Now, let us consider such self-energy diagrams in which one or more of the couplings y_b are replaced by the counterterm δy_b . The mass counterterm δm_b reads

$$\delta m_b = v_d \delta y_b = -\Sigma_b^{RL}(y_b + \delta y_b). \quad (19)$$

to all orders of the perturbative expansion and to leading order in $\tan \beta$. Let us denote the n -th order contribution to δy_b by $\delta y_b^{(n)}$. We can solve Eq. (19) recursively, by expressing $\delta y_b^{(n)}$ in terms of $\delta y_b^{(n-1)}$. Effectively $\delta y_b^{(n)}$ is simply computed from the one-loop diagrams contributing to Σ_b^{RL} including all possible substitutions of y_b by $\delta y_b^{(k)}$, $k = 1, \dots, n-1$. Adapting Eq. (10) and Eqs. (14–16) to account for the desired higher-order terms we write

$$\Sigma_b^{RL} = m_b^{(0)} \Delta_b = y_b^{(0)} v \epsilon_b \sin \beta. \quad (20)$$

Whenever Σ_b^{RL} is linear in $y_b^{(0)}$, that is if ϵ_b does not depend on $y_b^{(0)}$, one can easily determine δy_b to all orders: Noting that $y_b = m_b/v_d$ the one-loop result of Eq. (18) is replaced by

$$\delta y_b = -\frac{m_b}{v_d} [\epsilon_b \tan \beta - (\epsilon_b \tan \beta)^2 + (\epsilon_b \tan \beta)^3 - \dots] = -\frac{m_b}{v_d} \frac{\epsilon_b \tan \beta}{1 + \epsilon_b \tan \beta}. \quad (21)$$

If we discard the neutralino contribution and take $\epsilon_b^{\tilde{g}}$ and $\epsilon_b^{\tilde{\chi}^\pm}$ from Eqs. (15) and (16), we indeed find ϵ_b independent of y_b . There is a shortcut to Eq. (21): Adding $m_b = y_b v_d$ to both sides of Eq. (19) gives

$$v_d y_b^{(0)} = m_b - y_b^{(0)} v_d \epsilon_b \tan \beta \quad (22)$$

which is easily solved for $y_b^{(0)}$ resulting in the resummation formula of Ref. [21]:

$$y_b^{(0)} = \frac{m_b}{v_d(1 + \epsilon_b \tan \beta)}. \quad (23)$$

The linearity of $\epsilon_b^{\tilde{g}} + \epsilon_b^{\tilde{\chi}^\pm}$ in y_b beyond the decoupling limit appears to contradict the discussion in the Introduction, since the hedgehog diagrams of Fig. 2 contain any odd power of y_b . However, these additional factors of y_b are implicitly contained in the sbottom mass eigenstates $m_{\tilde{b}_{1,2}}$. From this observation it becomes clear that for the correct resummation of the $\tan \beta$ -enhanced corrections one must clearly state the renormalisation scheme for the supersymmetric parameters. Eq. (23) implies an on-shell scheme for the sbottom masses meaning here that $m_{\tilde{b}_{1,2}}$ are used as inputs. By contrast, many supersymmetric analyses use the diagonal elements of the mass matrix, $m_{\tilde{b}_{L,R}}$ and the μ parameter (entering the off-diagonal elements) as inputs. In this scheme y_b enters the problem explicitly via

the mass matrix and Eq. (23) is not correct. Similarly, Eq. (23) must also be modified if the sbottom mixing angle $\tilde{\theta}_b$ and the mixing phase $\tilde{\phi}_b$ are used as input parameters. These parameters are the natural choice for applications to collider physics, especially once the bottom squarks are discovered and their properties are to be studied. It is therefore of utmost importance to control the definition of $\tilde{\theta}_b$, in particular if constraints from low-energy data shall be combined with collider physics. We analyse this point in Sect. 2.2.

In summary, whenever \mathcal{M} does not suffer from $\cot \beta$ -suppression in the leading order, all $\tan \beta$ -enhanced corrections stem from δy_b . The dominant contributions from gluino and chargino loops can be resummed to all orders at the Lagrangian level, if an adequate scheme for the sbottom mass parameters is adopted. We stress that the resummed terms are local, so that one can reproduce the resummed effects from an effective Lagrangian. The effective $\bar{b}_L b_R H^0$, $\bar{b}_L b_R A^0$ and $\bar{t}_L b_R H^+$ couplings are simply obtained by replacing the tree-level Yukawa coupling with $y_b^{(0)}$ in Eq. (23). That is, the description of these couplings by an effective Lagrangian *does not* require any assumption on the size of M_{SUSY} : E.g. the use of Eq. (23) also correctly resums the $\tan \beta$ -enhanced corrections in high-energy collider processes, even if the momenta of the particles involved are of the order of M_{SUSY} . Further the results of Ref. [21] also extend to other couplings in the MSSM Lagrangian which are governed by y_b : Also in the higgsino couplings of the charginos and neutralinos the use of Eq. (23) correctly resums the enhanced corrections, irrespective of the sizes of the momenta and masses involved. The Feynman rules for these effective couplings are listed in Appendix C. However, the situation is different for a $\cot \beta$ -suppressed process: Here the enhanced one-loop correction depends on the kinematics of the studied process. For example, the coupling of the Standard-Model-like Higgs boson h^0 to fermions involves $\tan \beta$ -enhanced momentum-dependent one-loop form factors.

2.2 Sbottom mixing and resummation

As an introductory remark, we note that the resummation issue is simple if one interchanges the roles of y_b and m_b : Choosing δy_b as input will fix δm_b through Eq. (19), there are no enhanced corrections beyond one-loop order and any non-linear dependence of Σ_b^{RL} on y_b does not pose a problem. This avenue has been pursued in Sect. 2 of Ref. [21]. Yet in any phenomenological application we face the fact that we have precise data on m_b and not on y_b , so that we are stuck with the task to invert Eq. (22). We discuss this for three well-motivated schemes for the sbottom mass matrix here:

(i) **Input:** $m_{\tilde{b}_1}^2, m_{\tilde{b}_2}^2; \mu, \tan \beta$

If we express the sbottom mixing angle $\tilde{\theta}_b$ and phase $\tilde{\phi}_b$ in Eq. (11) through our input parameters, using relation (109), the bottom mass in Δ_b^g cancels and we find the gluino and chargino contributions to Σ_b^{RL} to be linear in y_b . This is the case used to illustrate the resummation in Eq. (21). If we assume the neutralino contributions to be linear in y_b , too, we arrive at

$$y_b^{(0)} = \frac{m_b}{v_d(1 + \Delta_b)}. \quad (24)$$

The chargino contribution $\Sigma_b^{RL, \tilde{\chi}^\pm} = m_b^{(0)} \Delta_b^{\tilde{\chi}^\pm}$ is always linear in y_b , it is not influenced by our choice of input parameters since no bottom squarks are involved. The neutralino contribution

$\Sigma^{RL, \tilde{\chi}^0} = m_b^{(0)} \Delta_b^{\tilde{\chi}^0}$ in (13) can be rewritten as

$$\begin{aligned} \Sigma_b^{RL, \tilde{\chi}^0} &= \frac{y_b g}{16\pi^2} \sum_{m=1}^4 \frac{m_{\tilde{\chi}_m^0}}{\sqrt{2}} \tilde{N}_{m2}^* \tilde{N}_{m3}^* \cdot B_0(m_{\tilde{\chi}_m^0}, m_{\tilde{b}_1}) \\ &\quad - \frac{y_b g}{16\pi^2} \sum_{m=1}^4 \frac{m_{\tilde{\chi}_m^0}}{\sqrt{2}} \tilde{N}_{m2}^* \tilde{N}_{m3}^* \sin^2 \tilde{\theta}_b \left(B_0(m_{\tilde{\chi}_m^0}, m_{\tilde{b}_1}) - B_0(m_{\tilde{\chi}_m^0}, m_{\tilde{b}_2}) \right), \end{aligned} \quad (25)$$

where the first line is linear in y_b , but the second line is found to contain terms of third order and higher in y_b after insertion of (109). In the decoupling limit $M_{\text{SUSY}} \gg v$, these higher order terms, which are proportional to $\sin^2 \tilde{\theta}_b \propto v^2/M_{\text{SUSY}}^2$, vanish and the neutralino contribution is correctly included into (24). For $M_{\text{SUSY}} \sim v$ on the other hand, the higher-order terms spoil the proper resummation because equation (19) cannot be solved analytically anymore. As $\Delta_b^{\tilde{\chi}^0}$ is small anyway, formula (24), though not entirely correct in this case, still holds to a very good approximation.

(ii) **Input:** $m_{\tilde{b}_1}^2, m_{\tilde{b}_2}^2; \tilde{\theta}_b, \tilde{\phi}_b$

Assuming that some day it will be possible to measure $\tilde{\theta}_b$ and $\tilde{\phi}_b$, we could take these quantities as our input instead of μ and $\tan \beta$. In Eqs. (11) and (13) $\Delta_b^{\tilde{g}}$ and $\Delta_b^{\tilde{\chi}^0}$ are directly given as a function of $\tilde{\theta}_b$ and $\tilde{\phi}_b$. Obviously, $\Sigma_b^{RL, \tilde{g}} = m_b^{(0)} \Delta_b^{\tilde{g}}$ does not exhibit any explicit y_b -dependence in this case, so that no reinsertion of δy_b into $\Sigma_b^{RL, \tilde{g}}$ is possible (it is absorbed into the physical mixing angle). The neutralino contribution $\Sigma_b^{RL, \tilde{\chi}^0}$ on the other hand is linear in y_b if we choose $\tilde{\theta}_b$ as input and it can be properly resummed now, in contrast to case (i). The modified relation between $y_b^{(0)}$ and m_b then reads

$$y_b^{(0)} = y_b + \delta y_b = \frac{m_b}{v_d} \frac{1 - \Delta_b^{\tilde{g}}}{1 + \Delta_b^{\tilde{\chi}^\pm} + \Delta_b^{\tilde{\chi}^0}}. \quad (26)$$

Note that this scheme does not involve an explicit $\tan \beta$ -enhanced counterterm to $\tilde{\theta}_b$. The implicit resummation encoded in a “measured” value of $\tilde{\theta}_b$ must, however, be taken into account in a proper analysis of the MSSM parameter space: In the large- $\tan \beta$ limit Eqs. (104) and (109) imply a correlation between $y_b^{(0)}$, μ and our input parameters:

$$e^{i\tilde{\phi}_b} \sin 2\tilde{\theta}_b = - \frac{2y_b^{(0)*} \mu v_u}{m_{\tilde{b}_1}^2 - m_{\tilde{b}_2}^2} \quad (27)$$

That is, in scheme (ii) μ inherits the large correction from $y_b^{(0)}$ because the product $y_b^{(0)*} \mu$ is fixed. Since μ enters the chargino and neutralino mass matrices $\mathcal{M}_{\tilde{\chi}^{\pm,0}}$, one should solve Eq. (27) for μ , use the value in $\tilde{\chi}^{\pm,0}$ and repeat the steps iteratively until Eqs. (26) and (27) are sufficiently (i.e. up to the neglected $\cot \beta$ -suppressed correction proportional to A_b) compatible. As a corollary we remark that a measurement of $m_{\tilde{b}_{1,2}}$, $\tilde{\theta}_b$ and μ (which can be inferred from chargino or neutralino masses) completely fixes $|y_b^{(0)}|$ through Eq. (27) if $\tan \beta$ is large. Once $|y_b^{(0)}|$ is known the coupling strengths of A^0 and H^0 to bottom quarks are fixed. $|y_b^{(0)}|$ enters the production cross sections of these particles and cannot be studied in A^0, H^0 decays to b quarks at the LHC because of the large $b\bar{b}$ background from QCD processes.

(iii) **Input:** $m_{\tilde{b}_L}^2, m_{\tilde{b}_R}^2; \mu, \tan \beta$

As the masses and mixing angles of the SUSY particles are not measured yet, this set is the most prominent one because its elements directly appear in the Lagrangian. In terms of these input parameters, the mixing angle can be expressed with the help of

$$e^{i\tilde{\phi}_b} \tan 2\tilde{\theta}_b = -\frac{2y_b^{(0)*} \mu v_u}{m_{\tilde{b}_L}^2 - m_{\tilde{b}_R}^2} \quad (28)$$

Since $\Delta_b^{\tilde{g}}$ is proportional to $\sin 2\tilde{\theta}_b = \tan 2\tilde{\theta}_b / (\sqrt{1 + \tan^2 2\tilde{\theta}_b})$ and in addition the squark masses appearing in the loop functions have to be replaced by $m_{\tilde{b}_L}^2$ and $m_{\tilde{b}_R}^2$ via (107), the y_b -dependence of $\Delta_b^{\tilde{g}}$ gets so complicated that (19) cannot be solved analytically anymore. This problem can be avoided in the following way: In a first approximation, we determine $m_{\tilde{b}_{1,2}}^2$ from (107) using the tree level value for y_b . Now we can calculate Δ_b as a function of the parameter set (i). In a next step, the resulting modified Yukawa coupling (24) can be reinserted into (107) to get corrected values for $m_{\tilde{b}_{1,2}}^2$. This procedure has to be repeated until the value of Δ_b converges. The resummed Yukawa coupling is then given by (24). Alternatively, we could calculate $\Delta_b^{\tilde{g}}$ and $\Delta_b^{\tilde{\chi}^0}$ iteratively as a function of the input parameters (ii), determining $\sin 2\tilde{\theta}_b$ from Eq. (28). In that case, Eq. (26) provides the resummed Yukawa coupling.

Eq. (24) has the same form as the widely-used relation between $y_b^{(0)}$ and m_b valid in the decoupling limit and quoted in Eq. (5). Therefore we will take parameter set (i) as the physical input from now on.

3 Flavour mixing at large $\tan \beta$

In the effective-field-theory approach the resummation of $\tan \beta$ -enhanced effects in flavour-changing transitions is achieved in the same way as in the flavour-conserving case: One calculates loop-induced couplings of H_u to quarks, now taking flavour mixing into account. After the Higgs doublets acquire their vevs the down-quark mass matrix is diagonalised. In the basis of quark mass eigenstates we face flavour-non-diagonal Yukawa couplings, as expected in a general 2HDM [22, 23, 30, 34]. This method is correct for $M_{\text{SUSY}} \gg v, M_{A^0, H^0, H^\pm}$. In this chapter we extend the resummation of $\tan \beta$ -enhanced effects to the case of any hierarchy between M_{SUSY} and v to cover the natural situation $M_{\text{SUSY}} \sim M_{A^0, H^0, H^\pm} \sim v$. First, our results allow us to assess the accuracy of the decoupling limit used in the literature. Second, we access a new field and calculate the $\tan \beta$ -enhanced loop corrections to genuine supersymmetric couplings: For instance, the gluino-quark-squark coupling, which is flavour-diagonal at tree-level, receives enhanced FCNC loop corrections just as the neutral Higgs bosons A^0 and H^0 do. These effective FCNC couplings of supersymmetric particles cannot be studied with the effective-field-theory approach, because these particles are treated as heavy and are integrated out.

Our diagrammatic treatment of $\tan \beta$ -enhanced loop corrections can easily be generalised to the flavour off-diagonal case. In the naive MFV framework, $\tan \beta$ -enhanced flavour transitions only arise from self-energies of down-type quarks involving chargino-squark exchange (see Fig. 4). In the case of d - s -transitions, the stop contribution is suppressed by $V_{ts}^* V_{td}$. Since we neglect the small Yukawa

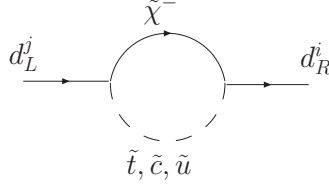
Figure 4: $\tan \beta$ -enhanced flavour-changing self-energy

Figure 5: Feynman diagrams with flavour-changing self-energy in an external leg.

couplings of up and charm and take degenerate masses for \tilde{u} and \tilde{c} squarks, the \tilde{u} and \tilde{c} contributions to d - s -transitions vanish because of a GIM cancellation. For the flavour-changing self-energies involving a bottom quark we find

$$\Sigma_{ij}^{RL}(V) = V_{ti}^* V_{tj} \frac{m_i \epsilon_{\text{FC}} \tan \beta}{1 + \epsilon_i \tan \beta}, \quad \text{for } (i, j) = (3, 1), (3, 2), (1, 3), (2, 3). \quad (29)$$

Here the unitarity of the CKM matrix and the mass degeneracy of the \tilde{u} and \tilde{c} squarks have been used to factor out the CKM combination $V_{ti}^* V_{tj}$. The explicit expression for ϵ_{FC} in terms of the stop mixing-parameters $\tilde{\theta}_t$, $\tilde{\phi}_t$ and the chargino mixing matrices \tilde{U} , \tilde{V} reads

$$\begin{aligned} \epsilon_{\text{FC}} = & -\frac{1}{16\pi^2} \frac{g}{\sqrt{2} M_W \sin \beta} \sum_{m=1}^2 m_{\tilde{\chi}_m^\pm} \tilde{U}_{m2}^* \left[\frac{y_t}{2} \tilde{V}_{m2}^* \sin 2\tilde{\theta}_t e^{i\tilde{\phi}_t} \left(B_0(m_{\tilde{\chi}_m^\pm}, m_{\tilde{t}_1}) - B_0(m_{\tilde{\chi}_m^\pm}, m_{\tilde{t}_2}) \right) \right. \\ & \left. - g \tilde{V}_{m1}^* \left(\cos^2 \tilde{\theta}_t B_0(m_{\tilde{\chi}_m^\pm}, m_{\tilde{t}_1}) + \sin^2 \tilde{\theta}_t B_0(m_{\tilde{\chi}_m^\pm}, m_{\tilde{t}_2}) - B_0(m_{\tilde{\chi}_m^\pm}, m_{\tilde{q}}) \right) \right], \end{aligned} \quad (30)$$

with $m_{\tilde{q}}$ denoting the common mass of the left-handed first and second generation squarks. If one wants to express ϵ_{FC} in terms of the SUSY-breaking parameters instead, one can use the relations given in Appendix A to find

$$\epsilon_{\text{FC}} = -\frac{y_t^2}{16\pi^2} A_t^* \mu^* (D_2 - |M_2|^2 D_0) + \frac{g^2}{16\pi^2} M_2^* \mu^* (D_2 - m_{\tilde{t}_R}^2 D_0 - C_0) \quad (31)$$

where $D_{0,2} = D_{0,2}(m_{\tilde{\chi}_1^\pm}, m_{\tilde{\chi}_2^\pm}, m_{\tilde{t}_1}, m_{\tilde{t}_2})$ and $C_0 = C_0(m_{\tilde{\chi}_1^\pm}, m_{\tilde{\chi}_2^\pm}, m_{\tilde{q}})$. Eq. (31) makes clear that ϵ_{FC} and thus also the $\tan \beta$ -enhanced flavour-changing self-energies are directly linked to the SUSY-breaking sector of the Lagrangian. They vanish if M_2 and A_t are set to zero. The part of ϵ_{FC} which is proportional to g^2 is absent if the left-right mixing of the top squarks is neglected and in addition universality for the mass terms of the left-handed squarks is assumed. We next present two different ways to account for ϵ_{FC} in practical calculations of low-energy flavour observables. The first option, explained in Sect. 3.1, is to consider self-energy corrections in external quark legs. The second possibility, discussed in Sect. 3.2, involves a flavour-non-diagonal wave-function renormalisation for the quark fields, which enters the Feynman rules of the couplings of quarks to SUSY particles and Higgs fields.

3.1 Flavour-changing self-energies in external legs

Consider the generic situation of a self-energy subdiagram in an external quark leg of some Feynman diagram, as displayed in Fig. 5 for the case of an external s quark. In flavour-conserving transitions such self-energies in external legs are truncated, they instead enter the S-matrix elements through the LSZ factor (“external wave-function renormalisation”). However, if the truncation affects a particle with a different mass than the external particle, the diagram with the external self-energy can be treated in the same way as a 1PI vertex correction [48], provided that the mass difference is much larger than the self-energy diagram. Despite of the $\tan \beta$ -enhancement, this condition, which reads $m_b - m_s \gg |\Sigma_{bs}|$ in our case, is certainly fulfilled because the self-energy Σ_{bs} is CKM-suppressed by a factor of $V_{ts}V_{tb}^*$. Treating external self-energies as 1PI diagrams makes the origin of the large effects most obvious. The alternative approach, which truncates all self-energies and introduces flavour-non-diagonal wave-function renormalisation, is discussed below in Sect. 3.2. Of course, both methods lead to the same results for physical amplitudes.

For definiteness we consider diagrams with external s or b quarks (Fig. 5). The case of $b \rightarrow d$ transitions is obtained by obvious replacements. For $m_s = 0$ the Feynman amplitudes are given by

$$\mathcal{M}_1 = \mathcal{M}_1^{\text{rest}} \cdot \frac{i(\not{p} + m_b)}{p^2 - m_b^2} \Big|_{\not{p}=0} (-i\Sigma_{bs}^{RL}) = -\mathcal{M}_1^{\text{rest}} \cdot V_{ts}V_{tb}^* \frac{\epsilon_{\text{FC}} \tan \beta}{1 + \epsilon_b \tan \beta}, \quad (32)$$

$$\mathcal{M}_2 = \mathcal{M}_2^{\text{rest}} \cdot \frac{i(\not{p} + m_s)}{p^2 - m_s^2} \Big|_{\not{p}=m_b^{\text{pole}}} (-i\Sigma_{bs}^{RL*}) = +\mathcal{M}_2^{\text{rest}} \cdot V_{ts}^*V_{tb} \frac{\epsilon_{\text{FC}}^* \tan \beta}{1 + \epsilon_b^* \tan \beta}. \quad (33)$$

Here, $\mathcal{M}_i^{\text{rest}}$ stands for the part of the Feynman amplitude corresponding to the truncated diagram. The expressions (32) and (33) are of order $\mathcal{O}(\epsilon_{\text{FC}} \tan \beta)$. Thus, if a large value of $\tan \beta$ compensates for the small ϵ_{FC} , it is possible to get a $b \rightarrow s$ transition without paying the price of a loop suppression.

There is one important physical process for which even diagrams with two self-energies in external lines must be considered: In $b \rightarrow s\gamma$ the expansion of the diagrams to lowest order in m_b/M_{SUSY} understood in Eqs. (32) and (33) gives zero. One therefore has to consider contributions of higher order in this ratio. This means that in Eq. (9) the right-hand side has to be expanded to order m_b^2/M_{SUSY}^2 in order to find the appropriate counterterm δm_b , whereas only the leading term was kept in chapter 2. We stress that this expansion does not spoil the resummation of the counterterm. Now let us have a look at the $b \rightarrow s\gamma$ -diagrams in Fig. 6. We observe that an insertion of δm_b like in the lower-left diagram (denoted by a cross) cancels only partially with a corresponding flavour-conserving self-energy insertion like in the upper-left diagram if we perform an on-shell calculation of the amplitude. The reason is that δm_b is determined at $p^2 = m_b^2$ while the self-energy is probed at $p^2 = 0$. The remnant is of order $\mathcal{O}(m_b^2/M_{\text{SUSY}}^2)$, just as the contribution that we find from the vertex correction in the upper-right diagram. For completeness, we mention that some non- $\tan \beta$ -enhanced contributions are canceled by insertions of on-shell wave-function counterterms of the bottom quark like the one shown in the lower-right diagram (also denoted by a cross). Summing up all the diagrams yields a gauge-invariant result of the order $(m_b/M_{\text{SUSY}})^2 \epsilon_{\text{FC}}^* \tan^2 \beta$ times another loop factor, which is the same order as the leading supersymmetric one-loop contribution to $b \rightarrow s\gamma$.

It is natural to ask whether the above effect, i.e. the generation of $\tan \beta$ -enhanced $b \rightarrow s$ transitions via self-energy insertions, also occurs for internal quark lines. It is important to notice that the $\tan \beta$ -enhancement in Eqs. (32) and (33) is generated by the fact that the quark propagator $-i/m_b$ cancels a factor of m_b in Σ_{bs}^{RL} . A potential $1/m_b$ -dependence of some loop integral would originate from the

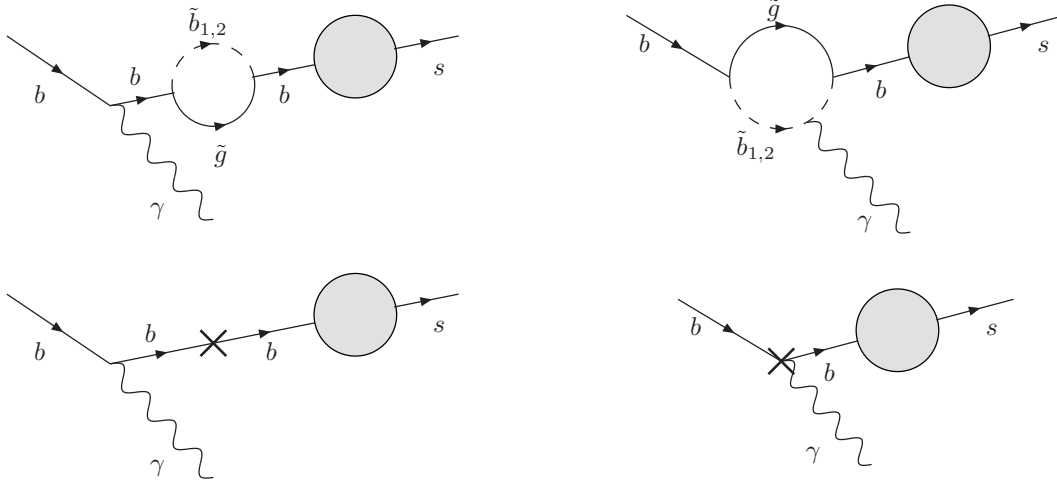


Figure 6: Some diagrams with self-energies in external lines for the process $b \rightarrow s\gamma$

low momentum region $p^2 \ll M_{SUSY}^2$, but we have constructed the mass counterterm δm_b in Section 2.1 in such a way that it subtracts the self-energy insertion in this momentum region. Therefore we only need to worry about situations similar to $b \rightarrow s\gamma$, in which higher orders of m_b/M_{SUSY} are relevant. However, we are not aware of a meaningful physical process in which an internal b line is responsible for a $1/m_b$ singularity in this way and do not consider this possibility further.

Before investigating the further consequences of the $\tan\beta$ -enhanced flavour transitions, we want to point out a subtlety of equation (33). The b -quark mass which enters the propagator via the equation of motion is the pole mass m_b^{pole} . The b -quark mass appearing in Σ_{bs}^{RL} , on the other hand, is the $\overline{\text{MS}}$ -mass m_b . However, if QCD-corrections to the diagrams of Fig. 5 are taken into account, additional contributions add to the $\overline{\text{MS}}$ -mass in Σ_{bs}^{RL} to give the pole mass m_b^{pole} . Therefore the b -quark mass correctly cancels from Eq. (33). A detailed analysis of this feature can be found in Appendix B.

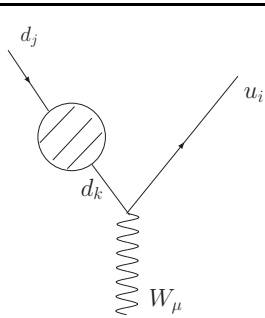


Figure 7: Generic $\tan\beta$ -enhanced correction to V_{ij}

Now, let us consider the $\tan\beta$ -enhanced corrections to the u_i - d_j - W -vertex (see Fig. 7). We apply an on-shell renormalisation condition to V_{ij} and cancel the contribution from the self-energy diagram at $p^2 = 0$ by a counterterm δV_{ij} . In this way the renormalised V corresponds to the CKM matrix measured from low energy data.² We find

$$\begin{aligned} \delta V_{ij} &= -V_{ik}\Lambda_{kj}, & \text{with} \\ \Lambda_{kj}(V) &= \begin{cases} \frac{m_{d_j}}{m_{d_j}^2 - m_{d_k}^2} \Sigma_{kj}^{LR} + \frac{m_{d_k}}{m_{d_j}^2 - m_{d_k}^2} \Sigma_{kj}^{RL} & , k \neq j \\ 0 & , k = j \end{cases} \end{aligned} \quad (34)$$

Note that δV_{ij} never involves less powers of the Wolfenstein parameter λ than V_{ij} . The bare CKM matrix $V^{(0)}$ reads

$$V^{(0)} = V + \delta V = V(1 - \Lambda) \approx V e^{-\Lambda}. \quad (35)$$

This shows that the chosen renormalisation condition preserves the unitarity of the CKM matrix because the matrix Λ is anti-hermitian.

From eq. (29) we find that the corrections δV_{td} , δV_{ts} , δV_{ub} and δV_{cb} are of order $\mathcal{O}(\epsilon_{\text{FC}} \tan\beta)$ and so can be comparable in size to the corresponding tree-level quantities V_{ij} . Hence, the situation is the

²Therefore our V corresponds to V^{eff} of Ref [35].

same as it was for the flavour-conserving self-energies in Section 2.1: Reinsertion of the counterterms δV_{ij} into the diagram of Fig. 7 leads to contributions which are formally of higher loop order but also of higher order in $\tan \beta$. To resum these corrections we generalise Eq. (34) to all orders in perturbation theory as

$$\delta V_{ij} = -(V_{ik} + \delta V_{ik}) \cdot \Lambda_{kj}(V + \delta V), \quad (36)$$

which is in complete analogy with eq. (19) for the flavour conserving case. Note that the enhanced flavour-conserving corrections associated with y_b are already properly resummed in Eq. (29) through the factor of $1/(1 + \epsilon_i \tan \beta)$. We have two possibilities to deal with Eq. (36). Firstly, we can expand the RHS order by order, deduce a recursive relation between the CKM counterterms $\delta V_{ij}^{(n)}$ and $\delta V_{ij}^{(n-1)}$ and perform the resummation explicitly. Secondly, we can add V_{ij} to both sides of Eq. (36) and solve the resulting matrix equation

$$V^{(0)} = V - V^{(0)} \cdot \Lambda(V^{(0)}) \quad (37)$$

for $V^{(0)}$. Inserting $\Lambda_{kj}(V^{(0)})$ from Eq. (34) with $\Sigma_{ij}^{RL} = \Sigma_{ji}^{LR*}$ from Eq. (29) into Eq. (37) yields

$$V_{ij}^{(0)} = V_{ij} - \sum_{k \neq j} V_{ik}^{(0)} V_{tk}^{(0)*} V_{tj}^{(0)} \frac{1}{m_j^2 - m_k^2} \left[\frac{m_j^2 \epsilon_{\text{FC}}^* \tan \beta}{1 + \epsilon_j^* \tan \beta} + \frac{m_k^2 \epsilon_{\text{FC}} \tan \beta}{1 + \epsilon_k \tan \beta} \right]. \quad (38)$$

Neglecting small quark mass ratios and ignoring the tiny corrections to the Cabibbo matrix we obtain the solution

$$V^{(0)} = \begin{pmatrix} V_{ud} & V_{us} & K^* V_{ub} \\ V_{cd} & V_{cs} & K^* V_{cb} \\ KV_{td} & KV_{ts} & V_{tb} \end{pmatrix}, \quad \text{with} \quad K = \frac{1 + \epsilon_b \tan \beta}{1 + (\epsilon_b - \epsilon_{\text{FC}}) \tan \beta}. \quad (39)$$

We recognise that this amounts to a renormalisation of the Wolfenstein parameter A ,

$$A^{(0)} = \left| \frac{1 + \epsilon_b \tan \beta}{1 + (\epsilon_b - \epsilon_{\text{FC}}) \tan \beta} \right| A. \quad (40)$$

Possible complex phases can be absorbed by the usual rephasing of the top-quark and bottom-quark fields (with the same phase for the left- and right-handed fields). In order to preserve supersymmetry, one should then perform the same rephasing also for the stop and sbottom fields.

Comparing Eq. (39) to results of calculations in effective-theory approaches [23, 25, 35, 36], where the SUSY particles are integrated out at a scale much higher than the electroweak scale, we see that the results are identical in the limit $M_{\text{SUSY}} \gg v$, as they should be. Yet our result Eq. (39) provides an explicit resummation of the $\tan \beta$ -enhanced flavour-changing effects to all orders in perturbation theory and is also valid in the case where the SUSY mass-scale is similar to the electroweak scale.

3.2 Renormalisation of the flavour-changing self-energies

The second possibility to deal with flavour-changing self-energies is to absorb them into wave-function counterterms. In this approach, no external-leg corrections have to be taken into account in the calculation of transition amplitudes. Instead, the effect of flavour-changing self-energies now resides in the wave-function counterterms, which enter the various couplings of the quark fields. In particular, the wave-function counterterms render couplings which are flavour-diagonal at tree-level

flavour-changing. Furthermore, this method permits an easy incorporation of the resummed $\tan \beta$ -enhanced effects into explicit Feynman rules for the MSSM. These Feynman rules are collected in Appendix C and can be readily implemented into computer programs like FeynArts [49,50]. They include for example flavour-changing gluino couplings, which have previously been found by Degrassi, Gambino and Slavich in Ref. [51]. We will see that these counterterm couplings are indeed enhanced by a factor of $\tan \beta$ and therefore determine them to all orders in the perturbative expansion, which has not been done in Ref. [51]. The scope of Ref. [51] is the calculation of the supersymmetric strong corrections to $b \rightarrow s\gamma$ for all values of $\tan \beta$, while we are interested in the leading power of $\tan \beta$ only, albeit to all orders in perturbation theory and with the effects of all gauge couplings and of the large Yukawa couplings y_t and y_b .

We next present the flavour-changing wave-function counterterms and reproduce the result for the renormalised CKM matrix of the previous section: The renormalisation of the CKM matrix with the help of wave-function counterterms has been first studied by Denner and Sack in Ref. [52] for the Standard Model, where an on-shell scheme has been chosen. That is to say, the wave-function counterterms have been defined in a proper way to cancel flavour-changing self-energies when one of the external quarks is put on the mass shell. Later Gambino, Grassi and Madricardo [53] have argued that this on-shell prescription can lead to gauge-noninvariant results and have given a renormalisation prescription for the flavour-changing two-point functions at zero external momentum p . As long as we neglect the external momenta in the calculation of the SUSY self-energy diagrams, there is no difference between the two approaches and the naive on-shell subtraction of flavour-changing self-energies in external quark legs gives gauge invariant results. Only chirality-flipping self-energies Σ_{ij}^{RL} in the down sector are $\tan \beta$ -enhanced. Therefore only down-quark fields have to be renormalised according to

$$d_{i,L}^{(0)} = \left(\delta_{ij} + \frac{1}{2} \delta Z_{ij}^L \right) d_{j,L}, \quad d_{i,R}^{(0)} = \left(\delta_{ij} + \frac{1}{2} \delta Z_{ij}^R \right) d_{j,R} \quad (41)$$

and their wave-function counterterms are anti-hermitian:

$$\delta Z_{ij}^L = -\delta Z_{ji}^{L*}, \quad \delta Z_{ij}^R = -\delta Z_{ji}^{R*}. \quad (42)$$

The wave-function renormalisation (41) corresponds to a unitary transformation of the down-type quark fields in flavour space. We will see in the following that this implies, in combination with a suitable renormalisation of the CKM matrix, that couplings of the Standard-Model particles to one another are unaffected by our renormalisation. In this way, no flavour violation occurs in the couplings of the photon, of the Z^0 boson, or of the gluon, as required by the decoupling theorem.

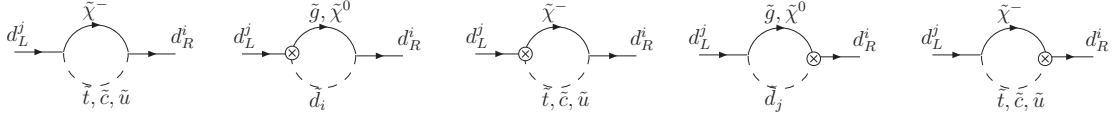
The rotation of the quark fields in Eq. (41) affects the down-quark mass terms of the Lagrangian (cf. Eq. (7)) as

$$\mathcal{L}_m = -m_{d_j}^{(0)} \bar{d}_{j,R}^{(0)} d_{j,L}^{(0)} + \text{h.c.} = - \left[m_{d_j}^{(0)} \delta_{jk} + \frac{1}{2} m_{d_j}^{(0)} \delta Z_{jk}^L - \frac{1}{2} m_{d_k}^{(0)} \delta Z_{jk}^R \right] \bar{d}_{j,R} d_{k,L} + \text{h.c.} \quad (43)$$

Subtraction of the flavour-changing self-energies at vanishing external momentum amounts to the condition

$$\Sigma_{ij}^{RL} + m_{d_i}^{(0)} \frac{\delta Z_{ij}^L}{2} - m_{d_j}^{(0)} \frac{\delta Z_{ij}^R}{2} = 0, \quad i \neq j, \quad (44)$$

for $\delta Z_{ij}^{L,R}$ with Σ_{ij}^{RL} given in (29). Here the bare masses $m_{d_i}^{(0)} = m_{d_i} + \delta m_{d_i}$ contain the $\tan \beta$ -enhanced corrections associated with the mass counterterms δm_{d_i} calculated in section 2.1.

Figure 8: Higher-order $\tan \beta$ -enhanced contributions to Σ_{ij}^{RL} .

The explicit expressions for the anti-hermitian one-loop counterterms in our scheme follow directly from the condition (44) and its complex-conjugate version. We find

$$\frac{\delta Z_{ij}^L}{2} = \frac{m_{d_i}^{(0)*} \Sigma_{ij}^{RL} + m_{d_j}^{(0)} \Sigma_{ij}^{LR}}{|m_{d_j}^{(0)}|^2 - |m_{d_i}^{(0)}|^2} \quad \text{for } i \neq j. \quad (45)$$

$$\frac{\delta Z_{ij}^R}{2} = \frac{m_{d_i}^{(0)} \Sigma_{ij}^{LR} + m_{d_j}^{(0)*} \Sigma_{ij}^{RL}}{|m_{d_j}^{(0)}|^2 - |m_{d_i}^{(0)}|^2} \quad \text{for } i \neq j. \quad (46)$$

From these formulae it is obvious that the counterterms $\delta Z_{ij}^{L,R}$ are $\tan \beta$ -enhanced. However, the strong hierarchy of the quark masses implies that δZ_{ij}^R is always suppressed by a small ratio of masses whereas δZ_{ij}^L is not.

We want to stress that in the expression for Σ_{ij}^{RL} in Eq. (29) the momenta of the external quarks are neglected. As a consequence self-energies in external quark lines are subtracted by the counterterms $\delta Z_{ij}^{L,R}$ only up to terms suppressed by the small ratio m_{d_i}/M_{SUSY} . Therefore in calculations where higher order terms in the momentum expansion are relevant one has to take into account the corresponding one-particle-reducible diagrams explicitly. One example for such a process is $b \rightarrow s\gamma$.

Up to now we have considered the flavour-changing self-energies only at the one-loop level. Are there also higher loop contributions which are $\tan \beta$ -enhanced? In the flavour-conserving case such contributions stem from insertions of the counterterm δy_b into the self-energy diagrams and are already included in Eq. (29). To study the new flavour-changing effects let us now consider self-energy diagrams with wave-function counterterms δZ_{ij}^L and δZ_{ij}^R at vertices involving a gluino, a chargino, or a neutralino. These diagrams generate further contributions to Σ_{ij}^{RL} (see Fig. 8). The resulting diagrams are $\tan \beta$ -enhanced and of the same order in the Wolfenstein parameter λ as the original flavour-changing chargino diagram. Formula (29) for Σ_{ij}^{RL} is then generalised to all orders in perturbation theory as

$$\Sigma_{ij}^{RL}(\delta Z_{ij}^L, \delta Z_{ij}^R) = V_{ti}^{(0)*} V_{tj}^{(0)} m_{d_i}^{(0)} \epsilon_{\text{FC}} \tan \beta + \frac{\delta Z_{ij}^L}{2} m_{d_i}^{(0)} \epsilon_i \tan \beta - \frac{\delta Z_{ij}^R}{2} m_{d_j}^{(0)} \epsilon_j \tan \beta. \quad (47)$$

In writing $V_{ij}^{(0)}$ we have anticipated that the CKM elements will obtain $\tan \beta$ -enhanced counterterms which then also should be included into the self-energies. Replacing Σ_{ij}^{RL} and Σ_{ij}^{LR} in Eqs. (45) and (46) by $\Sigma_{ij}^{RL}(\delta Z_{ij}^L, \delta Z_{ij}^R)$ and $\Sigma_{ij}^{LR}(\delta Z_{ij}^L, \delta Z_{ij}^R)$ gives us equations for the determination of the wave-function counterterms which are valid to all orders in the perturbative expansion. Again, they can be solved either order-by-order through explicit resummation or simply by solving the coupled equations for the resummed counterterms $\delta Z_{ij}^{L,R}$ obtained by inserting Eq. (47) into Eqs. (45) and (46). For

$i = d, s$ we find to leading order in m_{d_i}/m_b :

$$\frac{\delta Z_{bi}^L}{2} = -\frac{\delta Z_{ib}^{L*}}{2} = -\frac{\epsilon_{FC} \tan \beta}{1 + \epsilon_b \tan \beta} V_{tb}^{(0)*} V_{ti}^{(0)}, \quad (48)$$

$$\frac{\delta Z_{bi}^R}{2} = -\frac{\delta Z_{ib}^{R*}}{2} = -\frac{m_{d_i}}{m_b} \left[\frac{\epsilon_{FC} \tan \beta}{1 + \epsilon_b \tan \beta} + \frac{\epsilon_{FC}^* \tan \beta}{(1 + \epsilon_i^* \tan \beta)} \right] V_{tb}^{(0)*} V_{ti}^{(0)}. \quad (49)$$

The elements of $\delta Z_{ij}^{L,R}$ which do not involve the third generation vanish.

Now we can renormalise the CKM matrix with the help of the resummed left-handed wave-function counterterms, using the prescription of Ref. [52] and neglecting the up-type counterterms:

$$\delta V_{ij} = -\sum_k V_{ik}^{(0)} \frac{\delta Z_{kj}^L}{2} \quad (50)$$

On the right-hand side we have again replaced V_{ik} by $V_{ik}^{(0)}$ to properly account for the enhanced higher-order effects.

The resummed CKM counter-terms fixed by this condition exactly cancel the effect of the field renormalisation of the down-type quarks in their couplings to the W boson so that only the tree-level coupling survives. We can now insert Eq. (48) into Eq. (50) and (using $V_{ij}^{(0)} = V_{ij} + \delta V_{ij}$) solve for δV_{ij} . We obtain the same relation between $V_{ij}^{(0)}$ and V_{ij} as found in Eq. (39) with the method of the previous section. We may now express $\delta Z_{bi}^{L,R}$ in terms of the physical CKM elements: Inserting Eq. (39) into Eqs. (48) and (49) gives

$$\frac{\delta Z_{bi}^L}{2} = -\frac{\delta Z_{ib}^{L*}}{2} = -V_{tb}^* V_{ti} \frac{\epsilon_{FC} \tan \beta}{1 + (\epsilon_b - \epsilon_{FC}) \tan \beta}, \quad (51)$$

$$\frac{\delta Z_{bi}^R}{2} = -\frac{\delta Z_{ib}^{R*}}{2} = -V_{tb}^* V_{ti} \frac{m_{d_i}}{m_b} \left[\frac{\epsilon_{FC} \tan \beta}{1 + \epsilon_b \tan \beta} + \frac{\epsilon_{FC}^* \tan \beta}{(1 + \epsilon_i^* \tan \beta)} \right] \frac{1 + \epsilon_b \tan \beta}{1 + (\epsilon_b - \epsilon_{FC}) \tan \beta}. \quad (52)$$

The renormalisation of the CKM matrix beyond the decoupling limit has also been studied in the second chapter of Ref. [35], where an iterative procedure has been used to incorporate the $\tan \beta$ -enhanced higher-order corrections. We find that our unitary transformations in Eqs. (41) and (42) are formally equivalent to this procedure. Our result in Eq. (51) is the analytic expression for the limit to which the iterative calculation of Ref. [35] converges.

To summarise, in the previous section we found $\tan \beta$ -enhanced $b \rightarrow s$ ($b \rightarrow d$) transitions from self-energy insertions into external legs of Feynman diagrams. In the approach used in this section these self-energy insertions are absorbed into the wave-function counterterms.

3.3 Formulation of Feynman rules for the large- $\tan \beta$ scenario

We are now in a position to study the influence of $\tan \beta$ -enhanced flavour transitions on MSSM vertices by means of the counterterms defined above. In particular, we can give Feynman rules for the large- $\tan \beta$ framework in which the enhanced loop corrections are included and resummed to all orders.

First of all, as already stated above, we have chosen a renormalisation scheme such that the standard-model vertices remain unaffected by enhanced corrections. In the couplings of quarks to the neutral gauge bosons, the wave-function counterterms drop out by means of their antihermiticity. The W boson couplings are indeed affected by the field renormalisation but the renormalised CKM matrix is defined such that the coupling is given only by a physical matrix element V_{ij} . As an example, the coupling of the W to top- and strange-quark reads

$$-\frac{ig}{\sqrt{2}}\gamma_\mu P_L \left(V_{ts} + \delta V_{ts} + V_{tb} \frac{\delta Z_{bs}^L}{2} \right) = -\frac{ig}{\sqrt{2}}\gamma_\mu P_L V_{ts}. \quad (53)$$

Since we renormalise only the quark fields and not their superpartners, we cannot expect that the SUSY equivalents of standard-model vertices follow the same pattern. This is inevitable since the flavour-changing effects which we want to include in our Feynman rules arise from the SUSY-breaking sector (see Sect. 3). The most striking example for this property is the misalignment between the flavour-diagonal quark-gluon vertices and the quark-squark-gluino couplings which receive flavour-changing contributions. From the unitary transformations in Eq. (41) we can read off e.g.

$$\mathcal{L} \supset -i\sqrt{2}g_s T^a \tilde{b}_L^* \tilde{g}^a b_L^{(0)} = -i\sqrt{2}g_s T^a \tilde{b}_L^* \tilde{g}^a \left(b_L + \frac{\delta Z_{bs}^L}{2} s_L + \frac{\delta Z_{bd}^L}{2} d_L \right), \quad (54)$$

which implies the existence of a flavour-violating gluino coupling to a sbottom and a down- (strange-) quark via the $\tan \beta$ -enhanced counterterm $\delta Z_{bd(s)}^L$. In the approach of section 3.1, these corrections would arise via $\tan \beta$ -enhanced flavour-changing self-energies in the external quark line.

In addition to the gluino couplings, also chargino-, neutralino- and Higgs-couplings to quarks are affected by $\tan \beta$ -enhanced corrections. Moreover, the bare CKM factors in various flavour-changing squark couplings (not involving quarks) have to be related to their physical counterparts by means of Eq. (39). We summarise all these effects in explicit Feynman rules for the large- $\tan \beta$ scenario in Appendix C. These rules are useful for

- calculations of low-energy processes involving virtual SUSY particles and
- calculations in collider physics with external SUSY particles.

As an example, we give here the result for a flavour-changing gluino decay. In the approximation $m_b/M_{\text{SUSY}} \approx 0$, the decay rate of $\tilde{g} \rightarrow \tilde{b}_i b$ is at tree-level

$$\Gamma(\tilde{g} \rightarrow \tilde{b}_i b) = \frac{\alpha_s}{8\pi} (m_{\tilde{g}}^2 - m_{\tilde{b}_i}^2)^2. \quad (55)$$

For the flavour-violating decay $\tilde{g} \rightarrow \tilde{b}_i s$, we find

$$\frac{\Gamma(\tilde{g} \rightarrow \tilde{b}_i s)}{\Gamma(\tilde{g} \rightarrow \tilde{b}_i b)} = \left| \frac{\delta Z_{bs}^L}{2} \tilde{R}_{i1}^b \right|^2 + \left| \frac{\delta Z_{bs}^R}{2} \tilde{R}_{i2}^b \right|^2 \approx \left| \frac{\delta Z_{bs}^L}{2} \tilde{R}_{i1}^b \right|^2. \quad (56)$$

Numerically, this ratio is given by

$$\left| \frac{\epsilon_{\text{FC}} \tan \beta}{1 + (\epsilon_b - \epsilon_{\text{FC}}) \tan \beta} \right|^2 |V_{tb} V_{ts}|^2 |\tilde{R}_{i1}^b|^2 \sim \mathcal{O}(10^{-4}). \quad (57)$$

4 Phenomenology: FCNC processes

With the knowledge from the previous chapters one can now study the effects of $\tan\beta$ -enhanced SUSY corrections in FCNC processes. It is well known that even under the MFV assumption, supersymmetric contributions to FCNC observables in B physics can be sizeable if $\tan\beta$ is large. The most prominent example is the rare decay $B_s \rightarrow \mu^+ \mu^-$, in which the supersymmetric contribution can largely exceed the Standard-Model rate and can saturate the experimental bound [23, 24, 34–36, 41]. In this section we apply the effective Feynman rules for the large- $\tan\beta$ scenario listed in Appendix C to FCNC processes.

Most importantly, in this scenario flavour-changing transitions are no longer mediated exclusively by W bosons, charged Higgs particles and charginos but also by neutral Higgs particles, gluinos and neutralinos. For the case of the neutral Higgs bosons, this fact has been realised first in the framework of the effective 2HDM valid for $M_{\text{SUSY}} \gg v$ [22]. With our effective Feynman rules, we can on the one hand calculate the neutral Higgs contributions to FCNC processes for the case $M_{\text{SUSY}} \sim \mathcal{O}(v)$ and on the other hand derive contributions from other neutral virtual particles, where we will restrict the discussion to gluinos and neglect the weakly interacting neutralinos.

Since all the flavour-violating neutral couplings are generated by $\tan\beta$ -enhanced flavour-changing self-energies (or equivalently by the counterterms δZ_{bi}^L and δZ_{bi}^R ($i = d, s$) from Sect. 3.2), their numerical importance crucially depends on the parameter $\epsilon_{\text{FC}} \tan\beta$. Since δZ_{bi}^R is suppressed by a small ratio of quark masses, the most important new contributions are proportional to δZ_{bi}^L in Eq. (51) and thus to the parameter combination

$$\frac{\epsilon_{\text{FC}} \tan\beta}{1 + (\epsilon_b - \epsilon_{\text{FC}}) \tan\beta}. \quad (58)$$

It is thus useful to have a first estimate of the size of this parameter. For this purpose, we neglect the weak contributions to ϵ_b and ϵ_{FC} , focus on the non-decoupling part of expressions (15) and (31) for $\epsilon_b^{\tilde{g}}$ and ϵ_{FC} and set all the SUSY mass parameters as well as $|\mu|$ and $|A_t|$ equal to a single mass scale M_{SUSY} . In this case, the mass dependence drops out and we find

$$|\epsilon_{\text{FC}} \tan\beta| = \frac{y_t (M_{\text{SUSY}})^2}{32\pi^2} \tan\beta, \quad (59)$$

$$|(\epsilon_b - \epsilon_{\text{FC}}) \tan\beta| = |\epsilon_b^{\tilde{g}} \tan\beta| = \frac{\alpha_s (M_{\text{SUSY}})}{3\pi} \tan\beta. \quad (60)$$

For $\tan\beta = 50$ and $M_{\text{SUSY}} = 500$ GeV, we find typical numerical values of

$$|\epsilon_{\text{FC}} \tan\beta| \sim 0.12, \quad |(\epsilon_b - \epsilon_{\text{FC}}) \tan\beta| \sim 0.5. \quad (61)$$

Taking μ real here the parameter combination in Eq. (58) evaluates to

$$\left| \frac{\epsilon_{\text{FC}} \tan\beta}{1 + (\epsilon_b - \epsilon_{\text{FC}}) \tan\beta} \right| \sim 0.08, \quad \text{for positive } \mu, \quad (62)$$

$$\left| \frac{\epsilon_{\text{FC}} \tan\beta}{1 + (\epsilon_b - \epsilon_{\text{FC}}) \tan\beta} \right| \sim 0.24, \quad \text{for negative } \mu. \quad (63)$$

Values larger than this for ϵ_{FC} and thus for the combination (58) occur if $|A_t|$ is significantly larger than the masses of stops and charginos. If one requires $|A_t| \lesssim 3m_{\tilde{q}}$ (where $m_{\tilde{q}}$ is an average squark

mass) to avoid colour-breaking minima [54, 55], $\epsilon_{\text{FC}} \tan \beta$ gets constrained to $|\epsilon_{\text{FC}} \tan \beta|_{\text{max}} \sim 0.4$. Experimentally, the size of A_t is further limited by $\mathcal{B}(\overline{B} \rightarrow X_s \gamma)$ via the $\tan \beta$ -enhanced chargino contribution to this process. However, when the complex phase of A_t is taken into account, this bound is much weaker [56]. Moreover, this bound from $\mathcal{B}(\overline{B} \rightarrow X_s \gamma)$ may shift when the gluino contribution, which a priori is expected to be of order $|\epsilon_{\text{FC}} \tan \beta|$ times the chargino contribution, is taken into account.

4.1 The effective $|\Delta B| = 1$ Hamiltonian

Weak $|\Delta B| = |\Delta S| = 1$ decays are usually described by an effective Hamiltonian

$$\mathcal{H}_{\text{eff}} = -\frac{4G_F}{\sqrt{2}} V_{tb} V_{ts}^* \sum_i C_i \mathcal{O}_i + h.c. \quad (64)$$

In the SM the operator basis for radiative and hadronic B decays consists of the four quark operators

$$\mathcal{O}_1 = (\bar{s}_\alpha \gamma_\mu P_L c_\beta)(\bar{c}_\beta \gamma^\mu P_L b_\alpha) \quad \mathcal{O}_2 = (\bar{s}_\alpha \gamma_\mu P_L c_\alpha)(\bar{c}_\beta \gamma^\mu P_L b_\beta) \quad (65)$$

$$\mathcal{O}_3 = (\bar{s}_\alpha \gamma_\mu P_L b_\alpha) \sum_q (\bar{q}_\beta \gamma^\mu P_L q_\beta) \quad \mathcal{O}_4 = (\bar{s}_\alpha \gamma_\mu P_L b_\beta) \sum_q (\bar{q}_\beta \gamma^\mu P_L q_\alpha) \quad (66)$$

$$\mathcal{O}_5 = (\bar{s}_\alpha \gamma_\mu P_L b_\alpha) \sum_q (\bar{q}_\beta \gamma^\mu P_R q_\beta) \quad \mathcal{O}_6 = (\bar{s}_\alpha \gamma_\mu P_L b_\beta) \sum_q (\bar{q}_\beta \gamma^\mu P_R q_\alpha) \quad (67)$$

and the magnetic and chromo-magnetic operators

$$\mathcal{O}_7 = \frac{e}{16\pi^2} \bar{m}_b (\bar{s} \sigma^{\mu\nu} P_R b) F_{\mu\nu} \quad \mathcal{O}_8 = \frac{g_s}{16\pi^2} \bar{m}_b (\bar{s} \sigma^{\mu\nu} T^a P_R b) G_{\mu\nu}^a. \quad (68)$$

In the MSSM with large $\tan \beta$ flavour-changing couplings of the neutral Higgs bosons to the down-type quarks are generated. For this reason the operator basis has to be extended to include four quark operators with scalar, pseudoscalar and tensor structure, namely

$$\mathcal{O}_{11}^q = (\bar{s}_\alpha P_R b_\alpha)(\bar{q}_\beta P_L q_\beta) \quad \mathcal{O}_{12}^q = (\bar{s}_\alpha P_R b_\beta)(\bar{q}_\beta P_L q_\alpha) \quad (69)$$

$$\mathcal{O}_{13}^q = (\bar{s}_\alpha P_R b_\alpha)(\bar{q}_\beta P_R q_\beta) \quad \mathcal{O}_{14}^q = (\bar{s}_\alpha P_R b_\beta)(\bar{q}_\beta P_R q_\alpha) \quad (70)$$

$$\mathcal{O}_{15}^q = (\bar{s}_\alpha \sigma^{\mu\nu} P_R b_\alpha)(\bar{q}_\beta \sigma_{\mu\nu} P_R q_\beta) \quad \mathcal{O}_{16}^q = (\bar{s}_\alpha \sigma^{\mu\nu} P_R b_\beta)(\bar{q}_\beta \sigma_{\mu\nu} P_R q_\alpha). \quad (71)$$

Note that the operators $\mathcal{O}_{11}^q \dots \mathcal{O}_{16}^q$ are not linearly independent for $q = b$ or $q = s$. In these cases \mathcal{O}_{15}^q and \mathcal{O}_{16}^q can be expressed as linear combinations of the remaining operators using Fierz identities. We have checked that these operators have a negligible impact on radiative decays. The same feature was found for hadronic two-body decays in Ref. [57]. The effective Hamiltonian for $|\Delta B| = |\Delta D| = 1$ processes can be found from the $|\Delta B| = |\Delta S| = 1$ one by the replacement $s \rightarrow d$.

Let us now have a look at SUSY contributions to the Wilson coefficients of the operators \mathcal{O}_7 and \mathcal{O}_8 : In the SM $\mathcal{O}_{7,8}$ involves a chirality flip in the external b -quark leg so that $C_{7,8}$ is proportional to $m_b \propto \cos \beta$. Therefore SUSY contributions can be $\tan \beta$ -enhanced with respect to the SM amplitude if the chirality flip stems from a factor of y_b in the loop. At the one-loop level the well-known contributions growing with $\tan \beta$ are loops with charginos and up-type squarks. In this context often also the diagrams involving a charged Higgs boson and a top quark are discussed. These contributions are

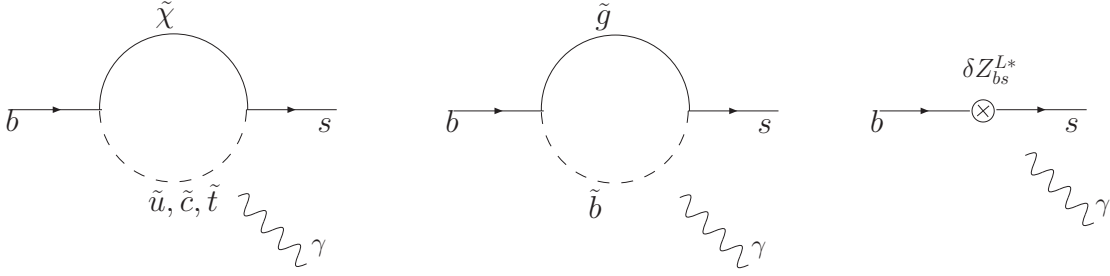


Figure 9: Gluino and chargino diagrams contributing to C_7 . The photon can couple to any particle except for the gluino. The contributions to C_8 are found by replacing the photon by a gluon (which can also couple to the gluino).

not $\tan \beta$ -enhanced due to the $\cos \beta$ -suppression of the charged-Higgs coupling to the right-handed top. Since this coupling has vertex-corrections proportional to $\sin \beta$, such diagrams require a different treatment and are not discussed here. They have been studied by various authors either in an effective-field-theory approach [38, 39, 58, 59] or in an explicit two-loop calculation [51]. Here we firstly focus on the chargino contribution. Using our effective Feynman rules we find

$$C_{7,8,\tilde{\chi}^\pm} = \frac{1}{\cos \beta (1 + \epsilon_b^* \tan \beta)} \sum_{a=1,2} \left\{ \frac{\tilde{U}_{a2} \tilde{V}_{a1} M_W}{\sqrt{2} m_{\tilde{\chi}_a^\pm}} \left[K^* f_{1,2}(x_{\tilde{q} \tilde{\chi}_a^\pm}) - c_{\tilde{t}}^2 f_{1,2}(x_{\tilde{t}_1 \tilde{\chi}_a^\pm}) - s_{\tilde{t}}^2 f_{1,2}(x_{\tilde{t}_2 \tilde{\chi}_a^\pm}) \right] + s_{\tilde{t}} c_{\tilde{t}} e^{-i\phi_{\tilde{t}}} \frac{\tilde{U}_{a2} \tilde{V}_{a2} m_t}{2 \sin \beta m_{\tilde{\chi}_a^\pm}} \left[f_{1,2}(x_{\tilde{t}_1 \tilde{\chi}_a^\pm}) - f_{1,2}(x_{\tilde{t}_2 \tilde{\chi}_a^\pm}) \right] \right\}. \quad (72)$$

with

$$s_{\tilde{t}} = \sin \tilde{\theta}_t, \quad c_{\tilde{t}} = \cos \tilde{\theta}_t, \quad x_{ij} = m_i/m_j. \quad (73)$$

All loop functions are given in appendix A.3. Again we have assumed that the squarks of the first two generations are degenerate in mass and denoted their common mass by $m_{\tilde{q}}$. Our result differs from the one in [39] only by a factor of K^* (defined in Eq. (39)) in the numerically small up and charm squark contribution. The stop contribution remains unaffected because the corrections from the wave function and the CKM counterterm cancel each other.

Besides the well-known chargino and charged-Higgs diagrams, there are now $\tan \beta$ -enhanced gluino-sbottom diagrams contributing to C_7 and C_8 (Fig. 9), which have never been discussed before in the context of minimal flavour-violation at large $\tan \beta$. Like the chargino diagrams these contributions vanish for $M_{\text{SUSY}} \gg v$, but can be computed with proper resummation of the enhanced corrections within our framework.

The $\tan \beta$ -enhanced parts read

$$C_{7,\tilde{g}} = \frac{\sqrt{2}}{4G_F} \frac{C_F g_s^2 \mu \tan \beta}{3m_{\tilde{g}}(m_{b_1}^2 - m_{b_2}^2)} \frac{\epsilon_{\text{FC}}^* \tan \beta}{(1 + \epsilon_b^* \tan \beta)(1 + (\epsilon_b^* - \epsilon_{\text{FC}}^*) \tan \beta)} \left(f_2(x_{b_1 \tilde{g}}) - f_2(x_{b_2 \tilde{g}}) \right), \quad (74)$$

$$C_{8,\tilde{g}} = - \frac{\sqrt{2}}{4G_F} \frac{g_s^2 \mu \tan \beta}{m_{\tilde{g}}(m_{b_1}^2 - m_{b_2}^2)} \frac{\epsilon_{\text{FC}}^* \tan \beta}{(1 + \epsilon_b^* \tan \beta)(1 + (\epsilon_b^* - \epsilon_{\text{FC}}^*) \tan \beta)} \times \left[C_F \left(f_2(x_{b_1 \tilde{g}}) - f_2(x_{b_2 \tilde{g}}) \right) + C_A \left(f_3(x_{b_1 \tilde{g}}) - f_3(x_{b_2 \tilde{g}}) \right) \right]. \quad (75)$$

The arguments of the loop functions are again given by $x_{ab} = m_a^2/m_b^2$, the colour factors are $C_F = 4/3$ and $C_A = 3$. We remark that the diagram with a gluino and a strange squark in the loop has been neglected because its amplitude is suppressed by the strange-quark mass. To have a rough estimate of the size of $C_{7,8,\tilde{g}}$ compared to $C_{7,8,\tilde{\chi}^\pm}$ we again set all SUSY masses (including $|\mu|$ and $|A_t|$) to the same value M_{SUSY} . In this case we find

$$\eta_7 = \left| \frac{C_{7,\tilde{g}}}{C_{7,\tilde{\chi}^\pm}} \right| = \frac{8}{15} \frac{g_s^2}{y_t^2} \frac{|\epsilon_{\text{FC}}^* \tan \beta|}{|1 + (\epsilon_b^* - \epsilon_{\text{FC}}^*) \tan \beta|}, \quad \eta_8 = \left| \frac{C_{8,\tilde{g}}}{C_{8,\tilde{\chi}^\pm}} \right| = \frac{10}{3} \frac{g_s^2}{y_t^2} \frac{|\epsilon_{\text{FC}}^* \tan \beta|}{|1 + (\epsilon_b^* - \epsilon_{\text{FC}}^*) \tan \beta|}. \quad (76)$$

Using our estimates for expression (58) we find $\eta_7 \sim 0.07$ and $\eta_8 \sim 0.42$ for positive values of μ and $\eta_7 \sim 0.2$ and $\eta_8 \sim 1.3$ for negative values of μ . It follows that the impact of the gluino contribution on C_7 is small (especially for positive μ) whereas the contribution to C_8 can be sizeable. Above we argued that the value of $|\epsilon_{\text{FC}} \tan \beta|$ can be increased up to $|\epsilon_{\text{FC}} \tan \beta| \sim 0.4$ if we choose large values for $|A_t|$. Of course, the size of $C_{7,8,\tilde{g}}$ gets larger for increasing values of $|\epsilon_{\text{FC}} \tan \beta|$. Note, however, that $C_{7,8,\tilde{\chi}^\pm}$ is proportional to A_t and thus the ratio $\eta_{7,8}$, i.e. the relative importance of the gluino contribution, is essentially unaffected. On the other hand, the gluino contribution grows with increasing $|\mu|$ whereas the chargino contribution decreases because it decouples with the chargino mass. Therefore for large values of $|\mu|$ the gluino contribution becomes more important. We will perform a more detailed numerical study of the new coefficients $C_{7,\tilde{g}}$ and $C_{8,\tilde{g}}$ in section 5.

Replacing in Fig. 9 the gluino by a neutralino, we find $\tan \beta$ -enhanced neutralino contributions to the (chromo-)magnetic operators. Their analytic expression reads

$$C_{7,\tilde{\chi}^0} = -\frac{\sqrt{2}}{4G_F} \sum_{i,m} \frac{\epsilon_{\text{FC}}^* \tan \beta}{6m_{\tilde{\chi}_m^0} m_b (1 + (\epsilon_b^* - \epsilon_{\text{FC}}^*) \tan \beta)} X_{im}^{L*} X_{im}^R f_2(x_{\tilde{b}_i \tilde{\chi}_m^0}) \quad , \quad C_{8,\tilde{\chi}^0} = 1/e_d C_{7,\tilde{\chi}^0} \quad (77)$$

with the neutralino-quark-squark couplings

$$X_{im}^L = \sqrt{2} \tilde{R}_{i1}^b \left(\frac{g}{2} \tilde{N}_{m2}^* - \frac{g'}{6} \tilde{N}_{m1}^* \right) - y_b^{(0)} \tilde{R}_{i2}^b \tilde{N}_{m3}^* \quad , \quad X_{im}^R = \frac{\sqrt{2}}{3} g' \tilde{R}_{i2}^b \tilde{N}_{m1} + y_b^{(0)*} \tilde{R}_{i1}^b \tilde{N}_{m3}. \quad (78)$$

In our convention, $e_d = -1/3$ is the charge of the down-type (s)quarks. The bare Yukawa coupling $y_b^{(0)}$ is determined as explained in section 2.2. We remark that in the product $X_{im}^{L*} X_{im}^R$, additional factors of $\tan \beta$ from sbottom-mixing and from $y_b^{(0)}$ are hidden, but nevertheless we find the neutralino contributions to be numerically small compared to their counterparts from chargino and gluino diagrams.

Another one-loop contribution to $C_{7,8}$, stemming from virtual neutral Higgs-bosons, has been presented in [7] in the effective-Lagrangian approach with vanishing SUSY CP-phases. In a full diagrammatic calculation, we find for these coefficients

$$C_{7,H^0} = -\frac{\epsilon_{\text{FC}}^* \tan \beta}{1 + (\epsilon_b^* - \epsilon_{\text{FC}}^*) \tan \beta} \frac{m_b^2 \tan^2 \beta}{36|1 + \epsilon_b \tan \beta|^2 m_{A^0}^2} \quad , \quad C_{8,H^0} = \frac{C_{7,H^0}}{e_d}. \quad (79)$$

In the decoupling limit, setting all SUSY phases to zero, this agrees with [7] up to the factor $1/e_d$. Compared to the other contributions from SM and MSSM particles, corrections from neutral-Higgs diagrams to $C_{7,8}$ are at most in the few-percent range.

In the following, let us leave the magnetic and chromomagnetic operators and discuss the remaining parts of the effective Hamiltonian. For the QCD-penguin operators \mathcal{O}_{3-6} , we find contributions from

gluino and neutralino loops to be small because of destructive interference of the two occurring internal squark flavours \tilde{b} and \tilde{s} . This is a remarkable difference to chargino loops, where this GIM-like cancellation is rather inefficient between the up-type squarks due to their very different Yukawa couplings. Furthermore, the usual power-suppression m_b^2/M_{SUSY}^2 is present and cannot be alleviated by a factor of $\tan \beta$ from the loop since no chirality flip is involved, in contrast to $\mathcal{O}_{7,8}$.

In the semileptonic decay $\bar{B} \rightarrow X_s \ell^+ \ell^-$, two semileptonic operators usually denoted by \mathcal{O}_9 and \mathcal{O}_{10} come into play. Chargino- and charged Higgs-diagrams contributing to these operators have been evaluated in [60] (we refer to this publication for the definition of $\mathcal{O}_{9,10}$) and it has been found that the corrections to the SM coefficients are small. Due to the GIM-like suppression described above, we find gluino and neutralino corrections to be even smaller.

The charged leptonic B decays $B_q^+ \rightarrow \ell^+ \nu_\ell$ ($q = d, s$) are dominated by tree-level diagrams with W boson, but may receive sizeable contributions from charged-Higgs exchange in the MSSM [27]. The charged Higgs boson couples to a right-handed b quark and (neglecting y_d and y_s) the only effect of $\tan \beta$ -enhanced corrections stems from K in Eq. (39) and $\epsilon_b \tan \beta$ in the Yukawa coupling in Eq. (23). The corresponding Feynman rule is given in Eq. (149). The same remark applies to the other charged-Higgs analyser $B \rightarrow D \tau \nu_\tau$ [28, 29].

Their neutral counterparts $B_q^0 \rightarrow \ell^+ \ell^-$ are loop-mediated, with a dramatic impact of a large value of $\tan \beta$. The phenomenologically most important decay in this class, $B_s^0 \rightarrow \mu^+ \mu^-$, is described by the effective Hamiltonian

$$\mathcal{H}_{\text{eff}} = -\frac{4G_F}{\sqrt{2}} V_{ts}^* V_{tb} \sum_{i=A,S,P} C_i \mathcal{O}_i + h.c. \quad (80)$$

with the operators

$$\mathcal{O}_A = (\bar{s} \gamma_\nu P_L b) (\bar{\mu} \gamma^\nu \gamma_5 \mu) \quad (81)$$

$$\mathcal{O}_S = \bar{m}_b (\bar{s} P_L b) (\bar{\mu} \mu) \quad (82)$$

$$\mathcal{O}_P = \bar{m}_b (\bar{s} P_L b) (\bar{\mu} \gamma_5 \mu). \quad (83)$$

At large $\tan \beta$, neutral Higgs exchange is known to be dominant since it occurs at tree-level in the effective theory at the electroweak scale [23], contributing to C_S and C_P .³ Making use of the flavour-changing neutral Higgs couplings from Appendix C, we can generalise the results in the literature to formulae which

- resum all $\tan \beta$ -enhanced mass- and wave-function renormalisation effects
- contain all possible complex phases from the SUSY breaking sector and
- do not resort to the decoupling limit $M_{\text{SUSY}} \gg v$.

Since the LHCb detector may soon precisely measure the $B_s \rightarrow \mu^+ \mu^-$ branching fraction, an improved treatment of the SUSY contribution to this decay is desirable now. With $m_{H^0}^2 = m_{A^0}^2$ in the

³The $\tan \beta$ -enhancement was found in a diagrammatic one-loop calculation in Ref. [41].

large- $\tan \beta$ limit, this Higgs-mediated contribution reads⁴

$$C_S = -C_P = -\frac{\epsilon_{\text{FC}}^* \tan \beta}{1 + (\epsilon_b^* - \epsilon_{\text{FC}}^*) \tan \beta} \frac{m_\mu \tan^2 \beta}{(1 + \epsilon_b^* \tan \beta)(1 + \epsilon_\mu \tan \beta) 2m_{A^0}^2}. \quad (84)$$

Here ϵ_μ is the analogue of ϵ_b for the muon (see e.g. [36, 42]).

4.2 The effective $|\Delta B| = 2$ Hamiltonian

In order to study the effects of $\tan \beta$ -enhanced flavour transitions in $B - \bar{B}$ oscillations, we write the $\Delta B = 2$ effective Hamiltonian as

$$\mathcal{H}_{\text{eff}} = \frac{G_F^2 m_W^2}{16\pi^2} (V_{tb}^* V_{tq})^2 \sum_i C_i \mathcal{O}_i \quad (85)$$

with $q = d, s$. The dimension-six operators \mathcal{O}_i are

$$\mathcal{O}^{VLL} = (\bar{b} \gamma_\mu P_L q) (\bar{b} \gamma^\mu P_L q), \quad (86)$$

$$\mathcal{O}_1^{LR} = (\bar{b} \gamma_\mu P_L q) (\bar{b} \gamma^\mu P_R q), \quad (87)$$

$$\mathcal{O}_2^{LR} = (\bar{b} P_L q) (\bar{b} P_R q), \quad (88)$$

$$\mathcal{O}_1^{SLL} = (\bar{b} P_L q) (\bar{b} P_L q), \quad (89)$$

$$\mathcal{O}_2^{SLL} = (\bar{b} \sigma_{\mu\nu} P_L q) (\bar{b} \sigma^{\mu\nu} P_L q) \quad (90)$$

and $\mathcal{O}^{VRR}, \mathcal{O}_1^{SRR}, \mathcal{O}_2^{SRR}$ which are obtained by replacing P_L by P_R .

Various contributions to $B - \bar{B}$ mixing have been obtained in the effective-theory approach in Refs. [22, 30, 33–36]. We specify to $B_s - \bar{B}_s$ mixing, which involves numerically important contributions proportional to m_s [30]. The first type of contributions to the Wilson coefficients of these operators which we want to consider are diagrams with neutral Higgs exchange analogous to the $B_s \rightarrow \mu^+ \mu^-$ diagram in the previous subsection. With our Feynman rules we find

$$C_1^{SLL} = -\frac{16\pi^2 m_b^2 \tan^2 \beta}{\sqrt{2} G_F M_W^2} \cdot \frac{\epsilon_{\text{FC}}^2 \tan^2 \beta}{(1 + \epsilon_b \tan \beta)^2 (1 + (\epsilon_b - \epsilon_{\text{FC}}) \tan \beta)^2} \cdot \mathcal{F}_-, \quad (91)$$

$$C_2^{LR} = -\frac{32\pi^2 m_b m_s \tan^2 \beta}{\sqrt{2} G_F M_W^2} \cdot \frac{|\epsilon_{\text{FC}} \tan \beta|^2}{|1 + \epsilon_b \tan \beta|^2 |1 + (\epsilon_b - \epsilon_{\text{FC}}) \tan \beta|^2} \cdot \mathcal{F}_+ \\ \times \left[1 + (1 - e^{2i\phi}) \frac{(\epsilon_b^* - \epsilon_{\text{FC}}^* - \epsilon_s^*) \tan \beta}{1 + \epsilon_s^* \tan \beta} \right] \quad (92)$$

$$\text{with } \phi = \arg \{ \epsilon_{\text{FC}} \tan \beta (1 + (\epsilon_b^* - \epsilon_{\text{FC}}^*) \tan \beta) \}. \quad (93)$$

Up to terms suppressed by $\tan^{-1} \beta$, we obtain here

$$\mathcal{F}_+ = \frac{2}{m_{A^0}^2}, \quad \mathcal{F}_- = 0. \quad (94)$$

⁴If $\tan \beta$ is small, Z-penguin and box diagrams become important. These contributions can be found in Ref. [61].

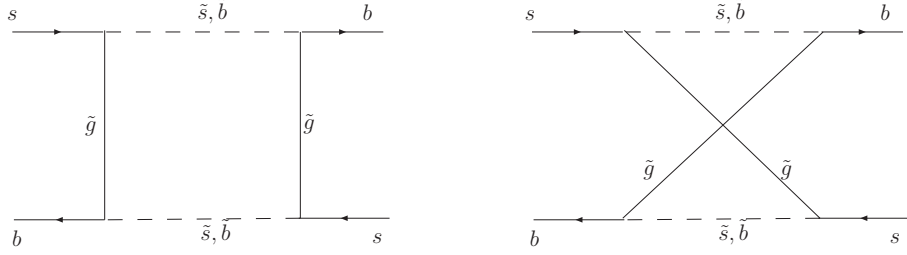


Figure 10: Gluino-box diagrams contributing to the $\Delta B = 2$ Hamiltonian. Two further diagrams are obtained by 90° rotations.

The contribution from the operator \mathcal{O}_2^{LR} is thus important despite its suppression by m_s since \mathcal{F}_- vanishes at large $\tan \beta$ [22]. Our result for C_2^{LR} involves the new term

$$r = (1 - e^{2i\phi}) \frac{(\epsilon_b^* - \epsilon_{FC}^* - \epsilon_s^*) \tan \beta}{1 + \epsilon_s^* \tan \beta}. \quad (95)$$

Obviously this correction factor r disappears if all parameters are real. It also vanishes if we go to the decoupling limit and choose all squark mass terms to be equal because in this case we have

$$\epsilon_s \rightarrow \epsilon_0, \quad \epsilon_b \rightarrow \epsilon_0 + \epsilon_{FC}. \quad (96)$$

For this reason the r -term is absent in [22, 30, 33–36]. Beyond the decoupling limit r does not vanish even if we set all SUSY-breaking mass terms to the same value because the squark masses are split due to electro-weak symmetry breaking. However, this effect is tiny for $\mu > 0$ where the correction factor $1/(1 + \epsilon_b \tan \beta)$ to the Yukawa coupling suppresses the off-diagonal element $X_{\tilde{b}} = -y_b^{(0)*} v_u \mu$ in the sbottom mass matrix. In this case we have $|r| \lesssim 0.01$. For $\mu < 0$ the off-diagonal element $X_{\tilde{b}}$ is enhanced and we have $|r| \lesssim 0.1$. Significantly larger values for r can be achieved if we allow the squark masses of the third generation to be different from those of the first two generations.⁵ In this case the new term can be important for mixing-induced CP asymmetries, because $|C_1^{SLL}|$ is much smaller than $|C_2^{LR}|$ (even after loop corrections to \mathcal{F}_- in Eq. (94) are included [36]) and the imaginary part of C_2^{LR} in Eq. (92) stems solely from r . A benchmark measurement of LHCb will be $A_{CP}^{\text{mix}}(\overline{B}_s \rightarrow (J/\psi\phi)_{CP\pm})$ which equals $\mp 0.04 \pm 0.01$ in the SM. In view of the smallness of this SM prediction the new contribution involving $\text{Im } r$ should be taken into consideration. The same remark applies to the even smaller SM prediction of the CP asymmetry in flavour-specific decays [48].

With our large- $\tan \beta$ Feynman rules we have further investigated the contributions to the $\Delta B = 2$ Hamiltonian from box-diagrams with virtual gluinos and down-type squarks depicted in Fig. 10. We find that contributions to $C_{1,2}^{LR}$, C^{VRR} and $C_{1,2}^{SRR}$ are always proportional to powers of δZ_{bs}^R , thus suppressed by m_s/m_b . Contributions to C^{VLL} and $C_{1,2}^{SLL}$ are proportional to $(\delta Z_{bs}^L)^2$, which is rather small as discussed at the beginning of Sect. 4, and furthermore suffer from destructive interference between the \tilde{s} and \tilde{b} contributions. These suppression effects render gluino contributions to the $\Delta B = 2$ Hamiltonian numerically negligible compared to other supersymmetric contributions like e.g. those from charginos or neutral Higgs bosons. The same statement holds for the neutralino box diagrams.

⁵It should be stressed that this is possible for the right-handed bilinear mass terms but not for the left-handed ones: In the super-CKM basis one has $\tilde{m}_{d_L}^2 = V^{(0)\dagger} \tilde{m}_{u_L}^2 V^{(0)}$ and the naive MFV hypothesis of diagonal $\tilde{m}_{d_L}^2$, $\tilde{m}_{u_L}^2$ matrices therefore implies $\tilde{m}_{u_L, d_L}^2 \propto \mathbb{1}$.

5 Numerical study of $C_{7,\tilde{g}}$ and $C_{8,\tilde{g}}$ and implications for $\bar{B}^0 \rightarrow \phi K_S$

We have argued in the previous sections that at large $\tan\beta$ there can be potentially large contributions to the coefficients of the (chromo-)magnetic $\Delta B = 1$ operators \mathcal{O}_7 and \mathcal{O}_8 from SUSY-QCD. In order to have a clearer picture of this effect, we now present a numerical study of the Wilson coefficients C_7 and C_8 and an application to the mixing-induced CP asymmetry $S_{\phi K_S}$.

As a first step, we have performed a general scan over the MSSM parameter space and calculated the absolute values and phases of the various standard-model and supersymmetric contributions to both C_7 and C_8 . Our ranges for the dimensionful MSSM parameters are given in Tab. 1. We vary the phase of A_t between 0 and 2π and $\tan\beta$ between 40 and 60. In this section we further take μ real and positive. Only parameter points compatible with the following constraints have been accepted:

- All squark masses are larger than 200 GeV.
- The lightest supersymmetric particle (LSP) is charge- and color-neutral.
- The experimental 2σ -bound on the lightest Higgs-boson mass is respected.
- $\mathcal{B}(\bar{B} \rightarrow X_s \gamma)$ is in the experimental 2σ -range.

For the last constraint, $\mathcal{B}(\bar{B} \rightarrow X_s \gamma)$ has been calculated according to Eq. (20) of Ref. [62]. This results in a severe limitation for large values of $|A_t|$ since $\mathcal{B}(\bar{B} \rightarrow X_s \gamma)$ is dominated by C_7 , which receives substantial SUSY corrections if both $|A_t|$ and $\tan\beta$ are large [63]. In view of this fact, the question arises how a complex A_t should be treated. It is often possible to fine-tune its phase in such a way that the sum of a very large SUSY correction to C_7 and the standard model value is still compatible with the measurements of $\mathcal{B}(\bar{B} \rightarrow X_s \gamma)$. We have decided to consider such a fine-tuning as unnatural and thus impose another constraint on our scan points.

- We reject all points yielding a SUSY correction $|C_7^{\text{SUSY}}(m_W)| > |C_7^{\text{SM}}(m_W)| \approx 0.22$

The results of the scan are depicted in Figs. 11 and 12. The plot in Fig. 11 is a comparison of the numerical importance of the well-known chargino contributions $C_{7,8,\tilde{\chi}^\pm}(\mu_{\text{SUSY}})$ on the one hand and the new gluino contribution $C_{7,8,\tilde{g}}(\mu_{\text{SUSY}})$ on the other hand. We show the absolute values of these (complex) Wilson coefficients. The picture confirms our rough estimate in Eq. (76), i.e. it shows that the gluino contribution to C_7 is accidentally suppressed, whereas it is enhanced for C_8 and can yield sizeable corrections, especially for large values of $|\mu|$. The different colours of the scan points correspond to different ranges of values for μ as indicated in the picture legend.

	min (GeV)	max (GeV)
$\tilde{m}_{Q_L}, \tilde{m}_{u_R}, \tilde{m}_{d_R}$	250	1000
$ A_t , A_b $	100	1000
μ, M_1, M_2	200	1000
M_3	300	1000
m_{A^0}	200	1000

Table 1: Scan ranges used for massive MSSM parameters.

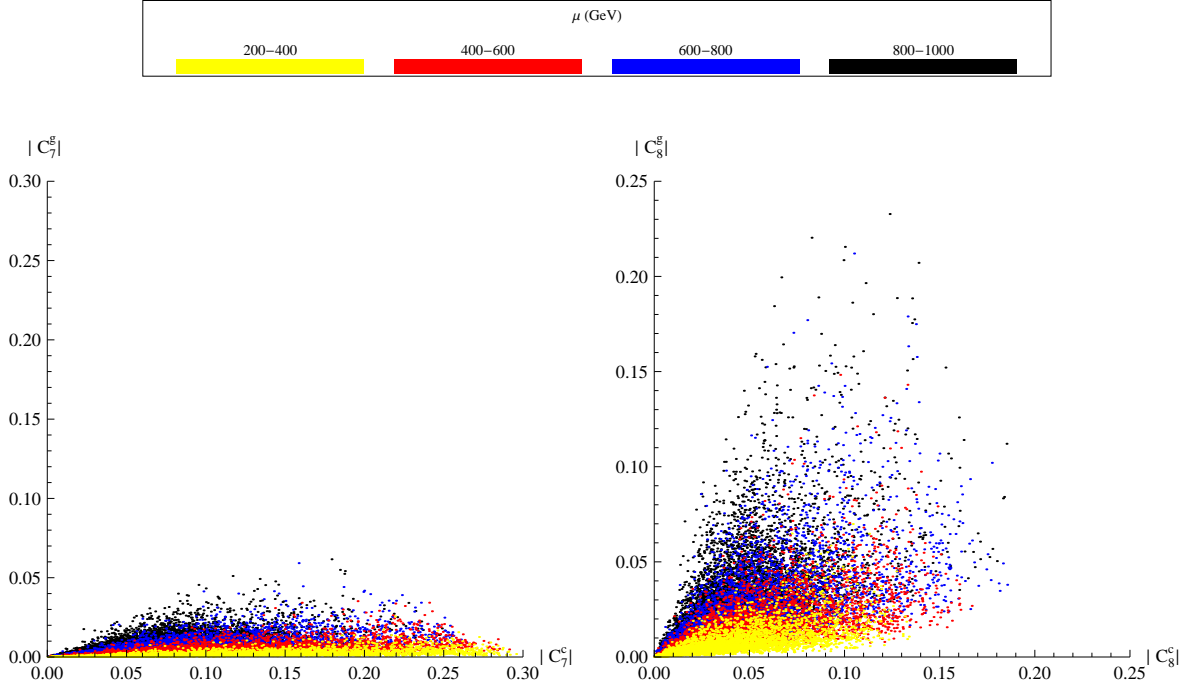


Figure 11: Magnitudes of chargino and gluino contributions to $C_7(\mu_{\text{SUSY}})$ and $C_8(\mu_{\text{SUSY}})$ scanned over the MSSM parameter space.

Next, in Fig. 12 we have plotted for each scan point in the parameter space the absolute values and phases of $C_7(m_b)$ and $C_8(m_b)$, including the SM and charged-Higgs contributions as well as the $\tan \beta$ -enhanced chargino contributions. The abscissa always represents our new value, taking into account also the gluino and neutralino contributions from Eqs. (74,75) and (77), while the ordinate represents the corresponding “old” value, discarding gluino-squark and neutralino-squark diagrams. In this way, the deviation from the diagonal indicates the relative size of the new contribution. In the Standard Model both coefficients are negative; we have plotted here $\arg(-C_{7,8})$ in order to center the phase plots around the origin.

We can see that the gluino-squark contributions do not cause strong modifications of $C_7(m_b)$, however they can have a strong impact on $C_8(m_b)$ for large values of μ . This confirms again the result of our estimate in section 4.1. The reason for the dependence of $C_8(m_b)$ on μ is the experimental constraint from $\mathcal{B}(\overline{B} \rightarrow X_s \gamma)$. The value of μ determines the mass of the higgsino component of the charginos. If $|\mu|$ is small, the higgsino is light and gives a potentially large contribution to $C_7(m_b)$ which is only compatible with data on $\mathcal{B}(\overline{B} \rightarrow X_s \gamma)$ if $|A_t|$ is rather small and the stops are rather heavy. As discussed above, this reduces in turn the value of ϵ_{FC} , to which the gluino contributions to the magnetic operators are proportional. Conversely, if $|\mu|$ is large, the higgsino is heavy and larger values of $|A_t|$ and ϵ_{FC} are possible. This feature is illustrated in Fig. 13 where we plot $|C_8(m_b)|$ over $|A_t|$ while fixing the other MSSM parameters to the values given in Tab. 2 and applying the same constraints as above. We see that a wide range of values is allowed for $|A_t|$ (this range corresponds to the plot range) and that the importance of the gluino-squark contributions to $|C_8(m_b)|$ grows with $|A_t|$.

Our finding affects some important low-energy observables which depend on $C_8(m_b)$. As an example, we have estimated the mixing-induced CP asymmetry $S_{\phi K_S}$ of the FCNC decay $\overline{B}^0 \rightarrow \phi K_S$. This

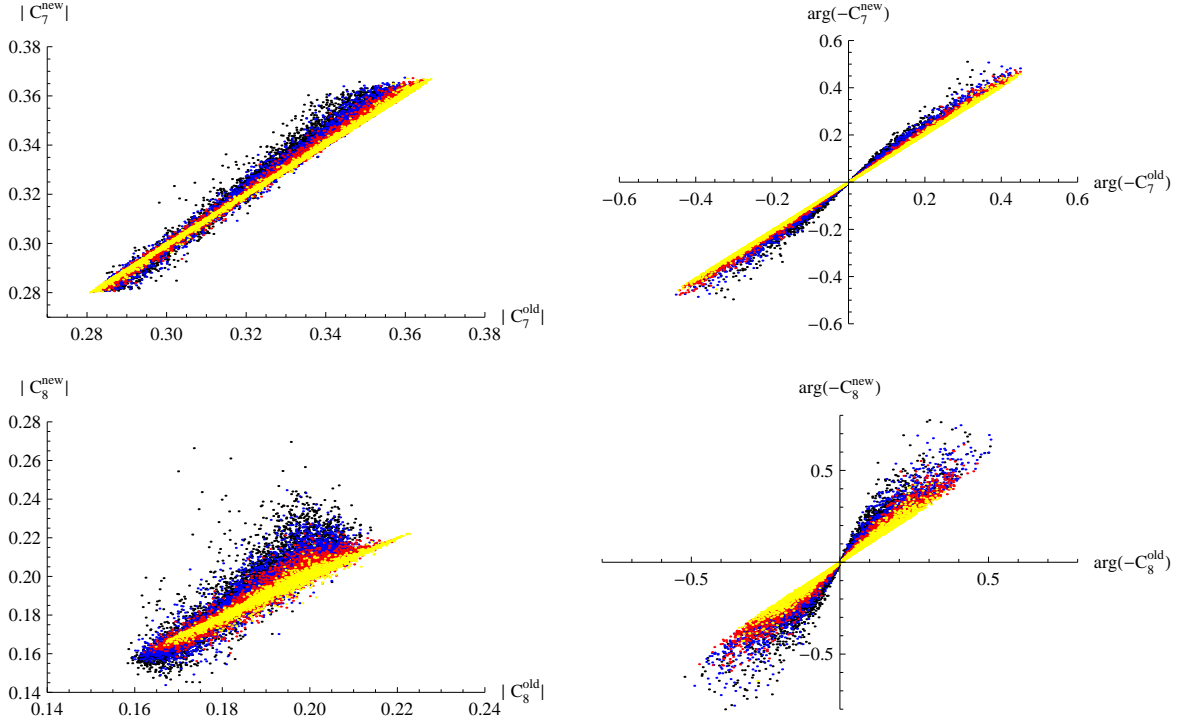


Figure 12: Magnitudes and phases of $C_7(m_b)$ and $C_8(m_b)$ scanned over the MSSM parameter space. The meaning of the colours is the same as in Fig. 11. For further details see text.

decay is generated by $b \rightarrow s \bar{s} s$ QCD penguins and can thus arise from the operator \mathcal{O}_8 with the gluon coupling to $\bar{s}s$. Here we only want to give a qualitative picture of the importance of the new contribution to the coefficient of \mathcal{O}_8 . Therefore we have calculated the matrix element only in the leading-order of QCD factorisation [64, 65], i.e. dropping $\mathcal{O}(\Lambda_{\text{QCD}}/m_b)$ and $\mathcal{O}(\alpha_s)$ corrections. Only the $\tan \beta$ -enhanced chargino and gluino contributions to $C_8(m_b)$ are taken into account and their sum is denoted by C_8^{NP} . The result presented here is therefore not to be seen as a precise quantitative prediction. A more detailed study including next-to-leading order effects will be performed in an upcoming publication.

For the moment, we will follow the analyses of Refs. [66] and [67] and write

$$\mathcal{A}_{\phi K_S} \equiv \langle \phi K_S | \mathcal{H}_{\text{eff}} | B^0 \rangle = A_{\phi K_S}^c [1 + a_{\phi K_S}^u e^{i\gamma} + (b_{\phi K_S}^c + b_{\phi K_S}^u e^{i\gamma}) C_8^{NP*}(m_W)] \quad (97)$$

for the $B^0 \rightarrow \phi K_S$ decay amplitude and $\bar{\mathcal{A}}_{\phi K_S}$ as the CP-conjugate \bar{B}^0 decay amplitude. We remark

$\tilde{m}_{Q_L}, \tilde{m}_{u_R}, \tilde{m}_{d_R}$	600 GeV	A_b	-600 GeV
μ	800 GeV	m_{A^0}	350 GeV
M_1	300 GeV	M_2	400 GeV
M_3	500 GeV	φ_{A_t}	$3\pi/2$
$\tan \beta$	50		

Table 2: Parameter point used for the numerical analyses of $C_8(m_b)$ in Fig. 13 and $S_{\phi K_S}$ in Fig. 14.

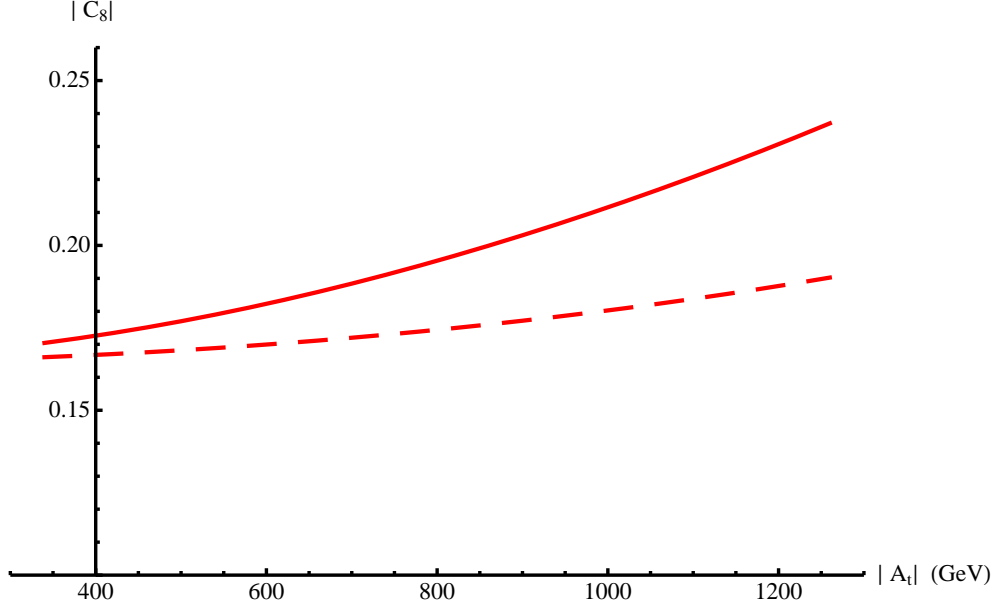


Figure 13: $|C_8(m_b)|$ as a function of $|A_t|$ for the parameter point of Tab. 2: full result (solid) and result without the gluino contribution (dashed).

that the complex conjugation of C_8^{NP} is missing in Ref. [67]. With the standard definition

$$\lambda_{\phi K_S} = -e^{-i\phi_B} \frac{\bar{\mathcal{A}}_{\phi K_S}}{\mathcal{A}_{\phi K_S}} \quad (98)$$

the mixing-induced CP asymmetry reads

$$S_{\phi K_S} = \frac{2 \operatorname{Im}(\lambda_{\phi K_S})}{1 + |\lambda_{\phi K_S}|^2}. \quad (99)$$

In this section we have not considered possible new-physics contributions to the phase ϕ_B of $B - \bar{B}$ mixing, which are necessarily small in our naive MFV scenario. We have found agreement with the numerical values of $a_{\phi K_S}^u$ and $b_{\phi K_S}^c$ in Ref. [66] and have used $b_{\phi K_S}^u \approx |V_{us}^* V_{ub}| / |V_{cs}^* V_{cb}| b_{\phi K_S}^c$. In Fig. 14 we plot $S_{\phi K_S}$ versus $|A_t|$ for the parameter point of Tab. 2. We can see a large impact of the gluino-squark contribution on $C_8^{NP}(m_b)$, especially for large $|A_t|$.

6 Conclusions

This paper addresses the MSSM for large values of $\tan \beta$. We have considered a version of Minimal Flavour Violation (MFV) in which all elementary couplings of neutral bosons to (s)quarks are flavour-diagonal and the flavour structures of W , charged-Higgs and chargino couplings are governed by the CKM matrix. Complex phases of flavour-conserving parameters like the trilinear SUSY-breaking term A_t are consistently included in our results. It is well-known that loop suppression factors can be compensated by a factor of $\tan \beta$, so that $\tan \beta$ -enhanced loop diagrams must be resummed to all orders in perturbation theory [4–6, 21, 25, 38, 42]. Further $\tan \beta$ -enhanced loop-induced FCNC couplings of neutral Higgs bosons lead to a plethora of interesting effects in B physics, which can

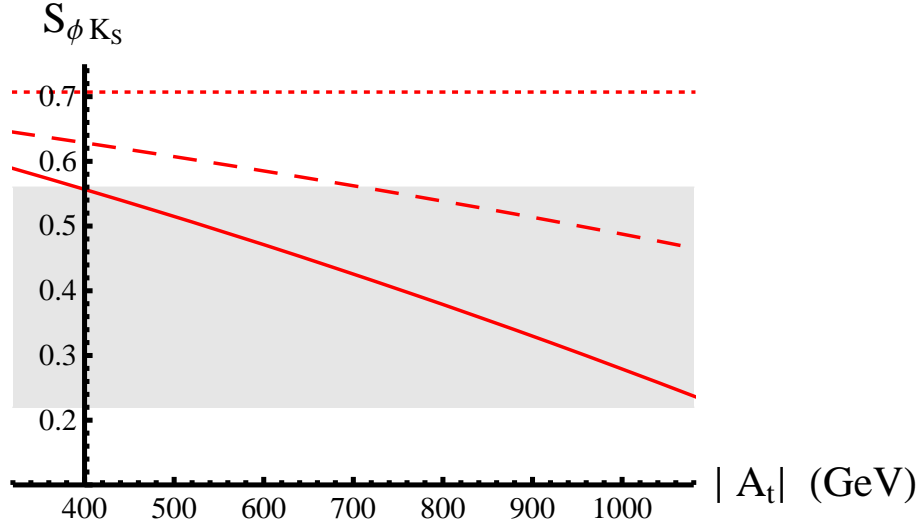


Figure 14: $S_{\phi K_S}$ as a function of $|A_t|$ at the parameter point of Tab. 2: full result (solid) and result without the gluino contribution (dashed). The shaded area represents the experimental 1σ range and the dotted line is the Standard-Model value.

be probed with current data from B factories and the Tevatron [7, 22–24, 30, 33–36, 68]. The subject is usually treated with the help of an effective field theory, a general two-Higgs-doublet model. This model is found by integrating out the genuine supersymmetric particles and is therefore valid for $M_{\text{SUSY}} \gg v, M_{A^0, H^0, H^\pm}$. In this paper we derive resummation formulae which do not assume any hierarchy between M_{SUSY} , the electroweak scale v and the Higgs masses. We use the diagrammatic resummation developed in Ref. [21] and extend the method to the case of flavour-changing interactions.

As a first result we derive the dependence of the resummation formula on the renormalisation scheme of the MSSM parameters. In particular we find that the familiar expression of Eq. (24) is modified if the sbottom mixing angle $\tilde{\theta}_b$ is used as input. This result is useful if high- p_T collider physics is studied in conjunction with low-energy data from B physics. While the focus of large- $\tan\beta$ collider physics has been on Higgs physics so far [20, 21, 69, 70], our result permits the correct treatment of $\tan\beta$ -enhanced effects in production and decay of bottom squarks. We then resum $\tan\beta$ -enhanced loop corrections to flavour-changing processes for arbitrary values of the supersymmetric particle masses. We find that the renormalisation of CKM elements and the loop-induced neutral-Higgs couplings to quarks have the same form as in the decoupling limit $M_{\text{SUSY}} \gg v, M_{A^0, H^0, H^\pm}$, but the loop-induced couplings depend on the supersymmetric parameters in a different way. As novel results we find $\tan\beta$ -enhanced loop-induced couplings of gluinos and neutralinos and determine the analogous corrections to chargino couplings. These results permit the study of $\tan\beta$ -enhanced corrections to processes involving a decoupling supersymmetric loop. Since these processes vanish for $M_{\text{SUSY}} \rightarrow \infty$, they cannot be studied with the effective-field-theory method employed in Refs. [7, 22, 23, 30, 33–36]. Other applications are flavour-changing processes with squark final states, which may be a topic for the ILC. All new FCNC couplings share a feature which was found for the flavour-conserving Higgs couplings to quarks in Ref. [21]: The resummed $\tan\beta$ -enhanced effects can be absorbed into judiciously chosen counterterms. Therefore they can be viewed as effective *local* couplings, irrespective of the hierarchy between M_{SUSY} and v . We exploit this feature to derive effective Feynman rules (collected in Appendix C) for all affected MSSM couplings. However, $\tan\beta$ -enhanced corrections

to suppressed tree-level couplings of order $\cot \beta$ are non-local and involve process-dependent form factors.

We have further performed an exhaustive phenomenological analysis of FCNC processes in B physics. The new gluino-squark loop contributions are negligible for $B - \bar{B}$ mixing and are small in $b \rightarrow s\gamma$, where they are of similar size as the non-enhanced two-loop contributions [51]. The latter feature stems from an accidental numerical suppression factor in the Wilson coefficient C_7 . This suppression is absent in C_8 : Here the gluino-squark loop can contribute as much as the known chargino-squark diagram. We have studied the impact on the mixing-induced CP asymmetry $S_{\phi K_S}$ in the decay $B_d \rightarrow \phi K_S$. The result in Fig. 14 complies with $\mathcal{B}(\bar{B} \rightarrow X_s \gamma)$ and the experimental lower bounds on the masses of sparticles and the lightest Higgs boson. Since no MSSM Higgs bosons are involved, the size of $S_{\phi K_S}$ is uncorrelated with $\mathcal{B}(B_s \rightarrow \mu^+ \mu^-)$. Therefore tighter future bounds on the latter quantity can be evaded by increasing M_{A^0} without suppressing $S_{\phi K_S}$. We have further generalised the known neutral-Higgs mediated contributions to $B_s \rightarrow \mu^+ \mu^-$ and $B_s - \bar{B}_s$ mixing to the case of arbitrary M_{SUSY} . Our more accurate expression for $\mathcal{B}(B_s \rightarrow \mu^+ \mu^-)$ is especially useful once LHCb measures this branching fraction in excess of the SM prediction. Finally we have identified a new contribution to $B_s - \bar{B}_s$ mixing: The parameter r in Eq. (95) can alter the phase of the $B_s - \bar{B}_s$ mixing amplitude and may affect the mixing-induced CP asymmetry in $B_s \rightarrow J/\psi \phi$.

Acknowledgements

The authors thank Andreas Crivellin for stimulating discussions and Wolfgang Altmannshofer for communications concerning Eq. (97). We further thank Leonardo Vernazza for helpful discussions on QCD factorisation and Thomas Hahn for checking eqs. (12,13). This work is supported by the DFG grant No. NI 1105/1–1, by project C6 of the DFG Research Unit SFB–TR 9 *Computergestützte Theoretische Teilchenphysik*, by the EU Contract No. MRTN-CT-2006-035482, “FLAVIANet”, and by BMBF grant no. 05H09VKF. L.H. and D.S. acknowledge the support by Ev. Studienwerk Villigst and by Cusanuswerk, respectively, and by the DFG Graduate College *High Energy Physics and Particle Astrophysics*.

A Conventions

Throughout this paper, our notation for SUSY parameters, sparticle masses and mixing matrices follows the conventions of the SLHA [43]. In Sect. A.1 we extend the SLHA to accommodate complex phases in the squark mass matrices. In Sect. A.2 we give explicit expressions for certain combinations of elements of the chargino mixing matrices. Sect. A.3 lists the loop functions entering our results.

A.1 Squark mixing

In the naive MFV scenario the squark mass-matrices are hermitian 2×2 -matrices. For top- and bottom-squarks they can be expressed in the basis $(\tilde{q}_L, \tilde{q}_R)$ with $q = t, b$ as

$$\mathcal{M}_{\tilde{q}}^2 = \begin{pmatrix} m_{\tilde{q}_L}^2 & X_{\tilde{q}} \\ X_{\tilde{q}}^* & m_{\tilde{q}_R}^2 \end{pmatrix}. \quad (100)$$

The diagonal elements can be chosen real and are given by

$$m_{\tilde{q}_L}^2 = \tilde{m}_{Q_L}^2 + m_q^2 + (T_q^3 - Q_q \sin^2 \theta_W) m_Z^2 \cos 2\beta, \quad (101)$$

$$m_{\tilde{q}_R}^2 = \tilde{m}_{q_R}^2 + m_q^2 + Q_q \sin^2 \theta_W m_Z^2 \cos 2\beta. \quad (102)$$

Neglecting terms proportional to the small v_d in the off-diagonal elements we obtain

$$X_{\tilde{t}} = m_t A_t^*, \quad (103)$$

$$X_{\tilde{b}} = -y_b^{(0)*} v_u \mu. \quad (104)$$

The mass eigenstates $\tilde{q}_{1,2}$ are related to the weak eigenstates via

$$(\tilde{q}_1, \tilde{q}_2)^T = \tilde{R}^q (\tilde{q}_L, \tilde{q}_R)^T \quad (105)$$

with a unitary matrix \tilde{R}^q which diagonalises the mass matrix:

$$\tilde{R}^q \mathcal{M}_q^2 \tilde{R}^{q\dagger} = \text{diag}(m_{\tilde{q}_1}^2, m_{\tilde{q}_2}^2), \quad (106)$$

$$m_{\tilde{q}_{1,2}}^2 = \frac{1}{2} \left(m_{\tilde{q}_L}^2 + m_{\tilde{q}_R}^2 \pm \sqrt{(m_{\tilde{q}_L}^2 - m_{\tilde{q}_R}^2)^2 + 4|X_q|^2} \right). \quad (107)$$

If the diagonal elements of the mass matrix are chosen real, the mixing matrix contains only one physical phase and can thus be parameterised as

$$\tilde{R}^q = \begin{pmatrix} \cos \tilde{\theta}_q & \sin \tilde{\theta}_q e^{i\tilde{\phi}_q} \\ -\sin \tilde{\theta}_q e^{-i\tilde{\phi}_q} & \cos \tilde{\theta}_q \end{pmatrix}, \quad (108)$$

i.e. by two real parameters, the mixing-angle $\tilde{\theta}_q$ and the phase $\tilde{\phi}_q$. In practical calculations where squarks are involved, elements of the mixing matrices appear in the Feynman rules. One then has the choice either to consider $\tilde{\theta}_q$ and $\tilde{\phi}_q$ as input parameters or to express them by means of the relation

$$e^{i\tilde{\phi}_q} \sin 2\tilde{\theta}_q = \frac{2X_{\tilde{q}}}{m_{\tilde{q}_1}^2 - m_{\tilde{q}_2}^2}, \quad (109)$$

that can be derived from eq. (106). To give separate relations for $\tilde{\theta}_q$ and $\tilde{\phi}_q$ one has to specify the allowed range for both parameters. Choosing $\tilde{\theta}_q \in [0, \pi/4]$ and $\tilde{\phi}_q \in [0, 2\pi)$ for example results in

$$\sin 2\tilde{\theta}_q = \left| \frac{2X_{\tilde{q}}}{m_{\tilde{q}_1}^2 - m_{\tilde{q}_2}^2} \right|, \quad \tilde{\phi}_q = \arg \left(\frac{2X_{\tilde{q}}}{m_{\tilde{q}_1}^2 - m_{\tilde{q}_2}^2} \right). \quad (110)$$

Constraining $\tilde{\theta}_q$ to this interval amounts to defining \tilde{q}_1 (\tilde{q}_2) as the eigenstate which is predominantly left-handed (right-handed).

We emphasize that in the sbottom mass-matrix we have defined the off-diagonal element $X_{\tilde{b}}$ in terms of the Yukawa coupling $y_b^{(0)}$ instead of the bottom mass. This parameterisation is valid irrespective of the renormalisation scheme used for the $\tan \beta$ -enhanced corrections to m_b . In practical calculations, one can use one of the resummation formulae given in section 2.1 to relate $y_b^{(0)}$ to the measured bottom mass. The corresponding corrections to m_b^2 in the diagonal elements of the sbottom mass-matrix are negligible since $m_b^2 \ll \tilde{m}_{Q_L}^2, \tilde{m}_{b_R}^2$.

A.2 Chargino mixing

In our conventions the chargino mass-matrix is given by

$$\mathcal{M}_{\tilde{\chi}^\pm} = \begin{pmatrix} M_2 & \sqrt{2}M_W \sin \beta \\ \sqrt{2}M_W \cos \beta & \mu \end{pmatrix}. \quad (111)$$

We define the biunitary transformation which brings it into diagonal form as

$$\tilde{U}^* \mathcal{M}_{\tilde{\chi}^\pm} \tilde{V}^\dagger = \text{diag}(m_{\tilde{\chi}_1^\pm}, m_{\tilde{\chi}_2^\pm}). \quad (112)$$

The matrices \tilde{U} and \tilde{V} can be determined by diagonalising the matrices $\mathcal{M}_{\tilde{\chi}^\pm}^\dagger \mathcal{M}_{\tilde{\chi}^\pm}$ and $\mathcal{M}_{\tilde{\chi}^\pm} \mathcal{M}_{\tilde{\chi}^\pm}^\dagger$. In Feynman amplitudes for diagrams with chirality-flipping propagators only certain combinations of matrix-elements of \tilde{U} and \tilde{V} appear. These combinations can be expressed as

$$\tilde{U}_{11} \tilde{V}_{11} = \frac{m_{\tilde{\chi}_1^\pm} M_2 - m_{\tilde{\chi}_2^\pm} \mu^* e^{i\psi}}{m_{\tilde{\chi}_1^\pm}^2 - m_{\tilde{\chi}_2^\pm}^2}, \quad \tilde{U}_{11} \tilde{V}_{12} = \sqrt{2}M_W \frac{m_{\tilde{\chi}_1^\pm} \sin \beta + m_{\tilde{\chi}_2^\pm} \cos \beta e^{i\psi}}{m_{\tilde{\chi}_1^\pm}^2 - m_{\tilde{\chi}_2^\pm}^2}, \quad (113)$$

$$\tilde{U}_{12} \tilde{V}_{12} = \frac{m_{\tilde{\chi}_1^\pm} \mu - m_{\tilde{\chi}_2^\pm} M_2^* e^{i\psi}}{m_{\tilde{\chi}_1^\pm}^2 - m_{\tilde{\chi}_2^\pm}^2}, \quad \tilde{U}_{12} \tilde{V}_{11} = \sqrt{2}M_W \frac{m_{\tilde{\chi}_1^\pm} \cos \beta + m_{\tilde{\chi}_2^\pm} \sin \beta e^{i\psi}}{m_{\tilde{\chi}_1^\pm}^2 - m_{\tilde{\chi}_2^\pm}^2}, \quad (114)$$

$$\tilde{U}_{21} \tilde{V}_{21} = \frac{m_{\tilde{\chi}_1^\pm} \mu^* e^{i\psi} - m_{\tilde{\chi}_2^\pm} M_2}{m_{\tilde{\chi}_1^\pm}^2 - m_{\tilde{\chi}_2^\pm}^2}, \quad \tilde{U}_{21} \tilde{V}_{22} = -\sqrt{2}M_W \frac{m_{\tilde{\chi}_1^\pm} \cos \beta e^{i\psi} + m_{\tilde{\chi}_2^\pm} \sin \beta}{m_{\tilde{\chi}_1^\pm}^2 - m_{\tilde{\chi}_2^\pm}^2}, \quad (115)$$

$$\tilde{U}_{22} \tilde{V}_{22} = \frac{m_{\tilde{\chi}_1^\pm} M_2^* e^{i\psi} - m_{\tilde{\chi}_2^\pm} \mu}{m_{\tilde{\chi}_1^\pm}^2 - m_{\tilde{\chi}_2^\pm}^2}, \quad \tilde{U}_{22} \tilde{V}_{21} = -\sqrt{2}M_W \frac{m_{\tilde{\chi}_1^\pm} \sin \beta e^{i\psi} + m_{\tilde{\chi}_2^\pm} \cos \beta}{m_{\tilde{\chi}_1^\pm}^2 - m_{\tilde{\chi}_2^\pm}^2} \quad (116)$$

with

$$e^{i\psi} = (M_2 \mu - M_W^2 \sin 2\beta) / (m_{\tilde{\chi}_1^\pm} m_{\tilde{\chi}_2^\pm}). \quad (117)$$

For large $\tan \beta$ the $\cos \beta$ -terms can be neglected and the above expressions reduce to

$$\tilde{U}_{11} \tilde{V}_{11} = \frac{M_2}{m_{\tilde{\chi}_1^\pm}} \cdot \frac{m_{\tilde{\chi}_1^\pm}^2 - |\mu|^2}{m_{\tilde{\chi}_1^\pm}^2 - m_{\tilde{\chi}_2^\pm}^2}, \quad \tilde{U}_{11} \tilde{V}_{12} = \frac{\sqrt{2}M_W m_{\tilde{\chi}_1^\pm} \sin \beta}{m_{\tilde{\chi}_1^\pm}^2 - m_{\tilde{\chi}_2^\pm}^2}, \quad (118)$$

$$\tilde{U}_{12} \tilde{V}_{12} = \frac{\mu}{m_{\tilde{\chi}_1^\pm}} \cdot \frac{m_{\tilde{\chi}_1^\pm}^2 - |M_2|^2}{m_{\tilde{\chi}_1^\pm}^2 - m_{\tilde{\chi}_2^\pm}^2}, \quad \tilde{U}_{12} \tilde{V}_{11} = \frac{M_2}{m_{\tilde{\chi}_1^\pm}} \cdot \frac{\sqrt{2}M_W \mu \sin \beta}{m_{\tilde{\chi}_1^\pm}^2 - m_{\tilde{\chi}_2^\pm}^2}, \quad (119)$$

$$\tilde{U}_{21} \tilde{V}_{21} = \frac{M_2}{m_{\tilde{\chi}_2^\pm}} \cdot \frac{|\mu|^2 - m_{\tilde{\chi}_2^\pm}^2}{m_{\tilde{\chi}_1^\pm}^2 - m_{\tilde{\chi}_2^\pm}^2}, \quad \tilde{U}_{21} \tilde{V}_{22} = -\frac{\sqrt{2}M_W m_{\tilde{\chi}_2^\pm} \sin \beta}{m_{\tilde{\chi}_1^\pm}^2 - m_{\tilde{\chi}_2^\pm}^2}, \quad (120)$$

$$\tilde{U}_{22} \tilde{V}_{22} = \frac{\mu}{m_{\tilde{\chi}_2^\pm}} \cdot \frac{|M_2|^2 - m_{\tilde{\chi}_2^\pm}^2}{m_{\tilde{\chi}_1^\pm}^2 - m_{\tilde{\chi}_2^\pm}^2}, \quad \tilde{U}_{22} \tilde{V}_{21} = -\frac{\mu}{m_{\tilde{\chi}_2^\pm}} \cdot \frac{\sqrt{2}M_W M_2 \sin \beta}{m_{\tilde{\chi}_1^\pm}^2 - m_{\tilde{\chi}_2^\pm}^2}. \quad (121)$$

A.3 Loop functions

In the calculation of quark self-energies with internal SUSY particles, we use the scalar integrals

$$B_0(m_1, m_2) = \frac{(2\pi\mu)^{4-d}}{i\pi^2} \int \frac{d^d q}{(q^2 - m_1^2)(q^2 - m_2^2)}, \quad (122)$$

$$C_0(m_1, m_2, m_3) = \frac{(2\pi\mu)^{4-d}}{i\pi^2} \int \frac{d^d q}{(q^2 - m_1^2)(q^2 - m_2^2)(q^2 - m_3^2)}, \quad (123)$$

$$D_0(m_1, m_2, m_3, m_4) = \frac{(2\pi\mu)^{4-d}}{i\pi^2} \int \frac{d^d q}{(q^2 - m_1^2)(q^2 - m_2^2)(q^2 - m_3^2)(q^2 - m_4^2)}, \quad (124)$$

where μ is the renormalisation scale. This corresponds to the well-known Passarino-Veltman notation with vanishing external momenta. Besides, we use the function

$$D_2(m_1, m_2, m_3, m_4) = \frac{(2\pi\mu)^{4-d}}{i\pi^2} \int \frac{q^2 d^d q}{(q^2 - m_1^2)(q^2 - m_2^2)(q^2 - m_3^2)(q^2 - m_4^2)}. \quad (125)$$

Explicit expressions for these integrals read

$$B_0(m_1, m_2) = \frac{2}{4-d} - \gamma_E + \log 4\pi + 1 - \log \frac{m_1^2}{\mu^2} + \frac{m_2^2}{m_2^2 - m_1^2} \log \frac{m_1^2}{m_2^2}, \quad (126)$$

$$C_0(m_1, m_2, m_3) = \frac{m_2^2}{(m_1^2 - m_2^2)(m_3^2 - m_2^2)} \log \frac{m_1^2}{m_2^2} + \frac{m_3^2}{(m_1^2 - m_3^2)(m_2^2 - m_3^2)} \log \frac{m_1^2}{m_3^2}, \quad (127)$$

$$D_0(m_1, m_2, m_3, m_4) = \frac{m_2^2}{(m_2^2 - m_1^2)(m_2^2 - m_3^2)(m_2^2 - m_4^2)} \log \frac{m_1^2}{m_2^2} + \frac{m_3^2}{(m_3^2 - m_1^2)(m_3^2 - m_2^2)(m_3^2 - m_4^2)} \log \frac{m_1^2}{m_3^2} + \frac{m_4^2}{(m_4^2 - m_1^2)(m_4^2 - m_2^2)(m_4^2 - m_3^2)} \log \frac{m_1^2}{m_4^2}, \quad (128)$$

$$D_2(m_1, m_2, m_3, m_4) = \frac{m_2^4}{(m_2^2 - m_1^2)(m_2^2 - m_3^2)(m_2^2 - m_4^2)} \log \frac{m_1^2}{m_2^2} + \frac{m_3^4}{(m_3^2 - m_1^2)(m_3^2 - m_2^2)(m_3^2 - m_4^2)} \log \frac{m_1^2}{m_3^2} + \frac{m_4^4}{(m_4^2 - m_1^2)(m_4^2 - m_2^2)(m_4^2 - m_3^2)} \log \frac{m_1^2}{m_4^2}. \quad (129)$$

The divergence in B_0 always drops out when we sum over the internal squarks and gauginos.

In our expressions for the Wilson coefficients $C_{7,8}$, we use the loop functions

$$f_1(x) = \frac{5-7x}{6(x-1)^2} + \frac{x(3x-2)}{3(x-1)^3} \log x, \quad (130)$$

$$f_2(x) = \frac{x+1}{2(x-1)^2} - \frac{x}{(x-1)^3} \log x, \quad (131)$$

$$f_3(x) = \frac{1}{2(x-1)} - \frac{x}{2(x-1)^2} \log x. \quad (132)$$

B QCD corrections to flavour-changing self-energies

Here we want to discuss the issue of the bottom mass appearing in calculations following the approach of Sect. 3.1. In that section, we have introduced $\tan \beta$ -enhanced flavour-mixing via flavour-changing



Figure 15: QCD corrections to the self-energy Σ_{bs}^{RL} (left) and the bottom mass m_b (right).

self-energies Σ_{bs}^{RL} in external legs. As a consequence the quark pole-mass m_b^{pole} enters the resulting expression through the Dirac equation $\not{p}b = m_b^{\text{pole}}b$. However, as we will show in this section, QCD corrections add in such a way that the final result does not depend on m_b^{pole} but only on the $\overline{\text{MS}}$ -mass m_b .

To see this we consider an effective theory at $\mu \sim \mathcal{O}(m_b)$ where the SUSY-particles are integrated out. The self-energy Σ_{bs}^{RL} then appears as Wilson coefficient of the (on-shell vanishing) operator $\bar{b}P_L s$. Comparing QCD corrections to this operator to QCD corrections to the bottom mass m_b (see Fig. 15) we find

$$\frac{\Sigma_{bs}^{RL(1)}(p)}{\Sigma_{bs}^{RL}} = \frac{\Sigma_b^{QCD}(p)}{m_b}, \quad (133)$$

where p denotes the external momentum. Therefore the Wilson coefficient Σ_{bs}^{RL} and the $\overline{\text{MS}}$ -mass m_b renormalise the same way. To make the behaviour under renormalisation explicit we write

$$\Sigma_{bs}^{RL} = m_b A \quad (134)$$

where now A is renormalisation-scale-independent (note the analogy to the definitions of ϵ_b and ϵ_{FC} in Eqs. (10), (14) and (29) which are thus renormalisation-scale independent).

Now we calculate QCD corrections to the diagrams in Fig. 5. Using the parameterisation (134) for Σ_{bs}^{RL} and neglecting the s-quark mass the Feynman amplitudes for the diagrams in figure 5 read

$$\mathcal{M}_1^{(1)} = \mathcal{M}_1^{\text{rest}} \cdot \frac{i(\not{p} + m_b)}{p^2 - m_b^2} \Big|_{\not{p}=0} (-i\Sigma_{bs}^{RL}) = -\mathcal{M}_1^{\text{rest}} \cdot A, \quad (135)$$

$$\mathcal{M}_2^{(2)} = \mathcal{M}_2^{\text{rest}} \cdot \frac{i(\not{p} + m_s)}{p^2 - m_s^2} \Big|_{\not{p}=m_b^{\text{pole}}} (-i\Sigma_{bs}^{RL*}) = +\mathcal{M}_2^{\text{rest}} \cdot A^* \frac{m_b}{m_b^{\text{pole}}}. \quad (136)$$

Since we want to perform a calculation up to order α_s in the effective theory we have to determine A from two-loop matching at the SUSY scale and we make this explicit by writing

$$A = A^{(0)} + A^{(1)} \quad (137)$$

where $A^{(1)}$ contains $\mathcal{O}(\alpha_s)$ QCD-corrections. The one-loop corrections to \mathcal{M}_1 and \mathcal{M}_2 in the effective theory are given in Figs. 16 and 17, respectively, with diagrams (1b) and (2b) taking into account the counterterm to the Wilson coefficient $\Sigma_{bs}^{RL} = m_b A$. As a consequence of (133), the contributions of (1a) and (1c) and of (1b) and (1d) cancel pairwise so that the expression for \mathcal{M}_1 in (135) still holds at one loop with $A = A^{(0)} + A^{(1)}$ instead of $A = A^{(0)}$. For the contributions of (2a) and (2b) we find with the help of (133)

$$\mathcal{M}_2^{(2a)} = \mathcal{M}_2^{\text{rest}} \cdot \frac{i(\not{p} + m_s)}{p^2 - m_s^2} \left(-i\Sigma_{bs}^{RL(1)*}(p) \right) \Big|_{\not{p}=m_b^{\text{pole}}} = \mathcal{M}_2^{\text{rest}} \cdot A^{(0)*} \frac{\Sigma_b^{QCD}(p)}{m_b^{\text{pole}}} \Big|_{\not{p}=m_b^{\text{pole}}} \quad (138)$$

$$\mathcal{M}_2^{(2b)} = \mathcal{M}_2^{\text{rest}} \cdot \frac{i(\not{p} + m_s)}{p^2 - m_s^2} \Big|_{\not{p}=m_b^{\text{pole}}} (-i\delta m_b A^{(0)*}) = \mathcal{M}_2^{\text{rest}} \cdot A^{(0)*} \frac{\delta m_b}{m_b^{\text{pole}}}. \quad (139)$$

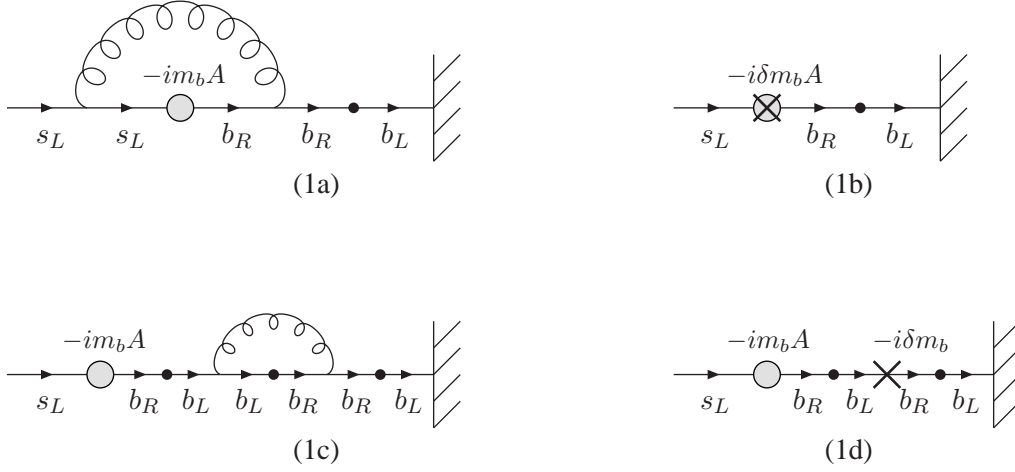


Figure 16: QCD corrections to diagram (1) in Fig. 5.

Adding these to Eq. (136) one gets

$$\mathcal{M}_2 = \mathcal{M}_2^{(2)} + \mathcal{M}_2^{(2a)} + \mathcal{M}_2^{(2b)} = \mathcal{M}_2^{\text{rest}} \cdot \frac{A^{(0)*}}{m_b^{\text{pole}}} \left(m_b + m_b \frac{A^{(1)*}}{A^{(0)*}} + \Sigma_b^{QCD}(p) \Big|_{\not{p}=m_b^{\text{pole}}} + \delta m_b \right). \quad (140)$$

Plugging in

$$m_b^{\text{pole}} = m_b + \Sigma_b^{QCD}(p) \Big|_{\not{p}=m_b^{\text{pole}}} + \delta m_b \quad (141)$$

and dropping terms of order $\mathcal{O}(\alpha_s^2)$ we get the final result

$$\mathcal{M}_2 = \mathcal{M}_2^{\text{rest}} \cdot (A^{(0)*} + A^{(1)*}) = \mathcal{M}_2^{\text{rest}} \cdot A^* \quad (142)$$

which now does not depend on m_b^{pole} anymore.

Applying this result to our case by expressing A in Eq. (142) through Σ_{bs}^{RL} via Eqs. (134) and (29) we find Eq. (33). Since Eq. (29) is linear in m_b , the parameterisation of Eq. (134) is quite natural. When one considers a more general Σ_{bs}^{RL} which is no longer linear in m_b (for example in the generic MSSM), the parameter A depends on m_b via (134) but in any case it does not involve m_b^{pole} .

C Feynman rules

In this appendix, we explain how $\tan \beta$ -enhanced loop corrections can be incorporated into calculations in the MSSM with naive MFV by simple modifications of the Feynman rules. The resulting modified rules are valid beyond the decoupling limit and refer to input scheme (i) for the sbottom parameters specified in section 2.1. They can also be used for processes with external SUSY particles. The modifications, which can easily be implemented into computer programs like FeynArts, are given as follows:

- (i) Express the Feynman rules in terms of the down-type Yukawa couplings y_{d_i} and replace them

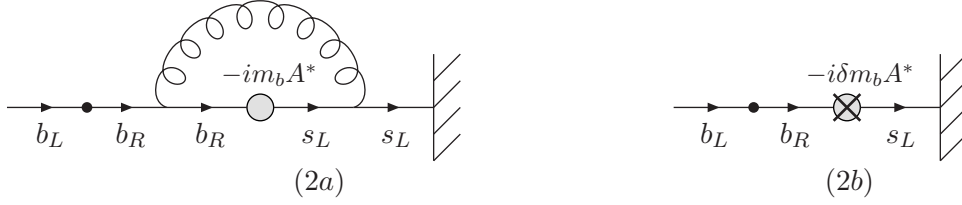


Figure 17: QCD corrections to diagram (2) in Fig. 5.

according to relation (24) by

$$y_{d_i} \rightarrow y_{d_i}^{(0)} = \frac{m_{d_i}}{v_d(1 + \epsilon_i \tan \beta)}. \quad (143)$$

It should be stressed that the same replacement has to be performed for the Yukawa coupling appearing in the sbottom mass matrix $\mathcal{M}_{\tilde{b}}$ in (100) before determining the mixing angle via (109). In case one wants to rely on input scheme (iii) the sbottom mixing matrix has to be calculated iteratively as described in section 2.2.

(ii) Replace CKM-elements involving the third quark generation according to

$$V_{ti} \rightarrow V_{ti}^{(0)} = \frac{1 + \epsilon_b \tan \beta}{1 + (\epsilon_b - \epsilon_{FC}) \tan \beta} V_{ti} \quad (i = d, s) \quad (144)$$

$$V_{ib} \rightarrow V_{ib}^{(0)} = \frac{1 + \epsilon_b^* \tan \beta}{1 + (\epsilon_b^* - \epsilon_{FC}^*) \tan \beta} V_{ib} \quad (i = u, c). \quad (145)$$

All other CKM-elements remain unchanged. The V_{ij} appearing after these replacements correspond to the physical ones which can be measured from the $W^+ u_i d_j$ -vertex.

(iii) This last rule concerns vertices involving down-type quarks. Into these one has to include the flavour-changing wave-function counterterms

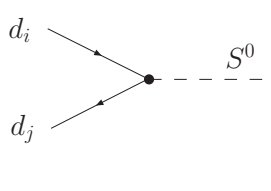
$$\frac{\delta Z_{bi}^L}{2} = -\frac{\epsilon_{FC} \tan \beta}{1 + \epsilon_b \tan \beta} V_{tb}^* V_{ti}^{(0)} \quad (146)$$

$$\frac{\delta Z_{bi}^R}{2} = -\frac{m_i}{m_b} \left[\frac{\epsilon_{FC} \tan \beta}{1 + \epsilon_b \tan \beta} + \frac{\epsilon_{FC}^* \tan \beta}{1 + \epsilon_i^* \tan \beta} \right] V_{tb}^* V_{ti}^{(0)} \quad (147)$$

for $i = d, s$. This leads to additional flavour-changing vertices and occasionally cancels the corrections from rule (ii).

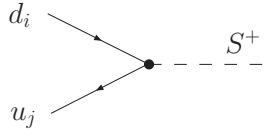
If one uses our Feynman rules, $\tan \beta$ -enhanced loop corrections of the form $(\epsilon \tan \beta)^n$ are automatically resummed to all orders. There is one exception: Proper vertex-corrections to the $\tan \beta$ -suppressed $h^0 d^i d^j$ - and $H^+ d_L^i u_R^j$ -vertices and to the corresponding Goldstone-boson vertices can not be accounted for by this method.

As mentioned above, additional flavour-changing vertices are generated by replacement rule (iii) in the case of external down-quarks. In the following we give explicit Feynman rules for these vertices, suppressing therein colour indices of (s)quarks. Repeated indices are not summed over.



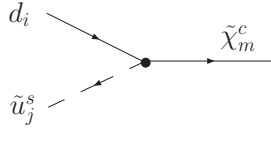
$$-\frac{i}{\sqrt{2}} \left[x_d^S \left(\delta_{ji} y_{d_j}^{(0)} + \frac{\delta Z_{ji}^L}{2} y_{d_j}^{(0)} - \frac{\delta Z_{ji}^R}{2} y_{d_i}^{(0)} \right) P_L \right. \\ \left. + (x_d^S)^* \left(\delta_{ji} y_{d_j}^{(0)*} + \frac{\delta Z_{ji}^R}{2} y_{d_j}^{(0)*} - \frac{\delta Z_{ji}^L}{2} y_{d_i}^{(0)*} \right) P_R \right] \quad (148)$$

with $x_d^S = (\cos \alpha, -\sin \alpha, i \sin \beta, -i \cos \beta)$ for $S^0 = (H^0, h^0, A^0, G^0)$

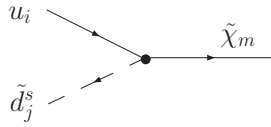


$$i \xi_L^S y_{u_j} V_{ji} P_L + i \xi_R^S \left(y_{d_i}^{(0)*} V_{ji}^{(0)} + \frac{\delta Z_{ji}^R}{2} y_{d_j}^{(0)*} V_{jj} \right) P_R \quad (149)$$

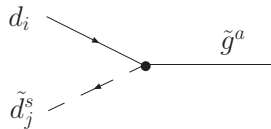
with $\xi_L^S = (\cos \beta, \sin \beta)$ and $\xi_R^S = (\sin \beta, -\cos \beta)$ for $S^+ = (H^+, G^+)$ (150)



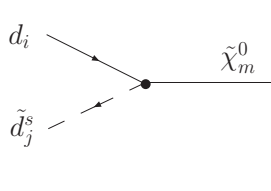
$$i V_{ji} \left(y_{u_j} \tilde{R}_{s2}^{u_j} \tilde{V}_{m2}^* - g \tilde{R}_{s1}^{u_j} \tilde{V}_{m1}^* \right) P_L \\ + i \tilde{R}_{s1}^{u_j} \tilde{U}_{m2} \left(y_{d_i}^{(0)*} V_{ji}^{(0)} + \frac{\delta Z_{ji}^R}{2} y_{d_j}^{(0)*} V_{jj} \right) P_R \quad (151)$$



$$i V_{ij}^{(0)*} \left[\left(y_{d_j}^{(0)} \tilde{R}_{s2}^{d_j} \tilde{U}_{m2}^* - g \tilde{R}_{s1}^{d_j} \tilde{U}_{m1}^* \right) P_L + y_{u_i} \tilde{R}_{s1}^{d_j} \tilde{V}_{m2} P_R \right] \quad (152)$$

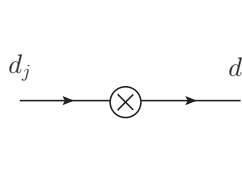


$$-i \sqrt{2} g_s T^a \left[\left(\delta_{ji} + \frac{\delta Z_{ji}^L}{2} \right) \tilde{R}_{s1}^{d_j} P_L - \left(\delta_{ji} + \frac{\delta Z_{ji}^R}{2} \right) \tilde{R}_{s2}^{d_j} P_R \right] \quad (153)$$



$$i \left(\delta_{ji} + \frac{\delta Z_{ji}^L}{2} \right) \left[\sqrt{2} \tilde{R}_{s1}^{d_j} \left(\frac{g}{2} \tilde{N}_{m2}^* - \frac{g'}{6} \tilde{N}_{m1}^* \right) - y_{d_j}^{(0)} \tilde{R}_{s2}^{d_j} \tilde{N}_{m3}^* \right] P_L \\ - i \left(\delta_{ji} + \frac{\delta Z_{ji}^R}{2} \right) \left[\frac{\sqrt{2}}{3} g' \tilde{R}_{s2}^{d_j} \tilde{N}_{m1} + y_{d_j}^{(0)*} \tilde{R}_{s1}^{d_j} \tilde{N}_{m3} \right] P_R \quad (154)$$

Occasionally, the flavour-changing counterterms have to be explicitly inserted into external or internal quark lines. In these cases, they cancel insertions of $\tan \beta$ -enhanced flavour-changing self-energies up to corrections which are suppressed by at least one power of m_b/M_{SUSY} . The Feynman rule reads



$$-i \left(\frac{m_i}{1 + \epsilon_i \tan \beta} \frac{\delta Z_{ij}^L}{2} - \frac{m_j}{1 + \epsilon_j \tan \beta} \frac{\delta Z_{ij}^R}{2} \right) P_L \\ -i \left(\frac{m_i}{1 + \epsilon_i^* \tan \beta} \frac{\delta Z_{ij}^R}{2} - \frac{m_j}{1 + \epsilon_j^* \tan \beta} \frac{\delta Z_{ij}^L}{2} \right) P_R. \quad (155)$$

References

- [1] **Muon G-2** Collaboration, G. W. Bennett *et. al.*, *Final report of the muon E821 anomalous magnetic moment measurement at BNL*, *Phys. Rev.* **D73** (2006) 072003, [hep-ex/0602035].
- [2] M. Davier: *Measurement of the Cross Section $e^+e^- \rightarrow \pi^+\pi^-\gamma$ (FSR) from Threshold to 4 GeV Using Radiative Return with BaBar*, Talk at “Tau’08”, Novosibirsk, Russia, September 22-25, 2008, <http://tau08.inp.nsk.su/talks/24/Davier.ppt>.
- [3] T. Banks, *Supersymmetry and the Quark Mass Matrix*, *Nucl. Phys.* **B303** (1988) 172.
- [4] L. J. Hall, R. Rattazzi, and U. Sarid, *The Top quark mass in supersymmetric SO(10) unification*, *Phys. Rev.* **D50** (1994) 7048–7065, [hep-ph/9306309].
- [5] R. Hempfling, *Yukawa coupling unification with supersymmetric threshold corrections*, *Phys. Rev.* **D49** (1994) 6168–6172.
- [6] M. S. Carena, M. Olechowski, S. Pokorski, and C. E. M. Wagner, *Electroweak symmetry breaking and bottom - top Yukawa unification*, *Nucl. Phys.* **B426** (1994) 269–300, [hep-ph/9402253].
- [7] G. D’Ambrosio, G. F. Giudice, G. Isidori, and A. Strumia, *Minimal flavour violation: An effective field theory approach*, *Nucl. Phys.* **B645** (2002) 155–187, [hep-ph/0207036].
- [8] G. Colangelo, E. Nikolidakis, and C. Smith, *Supersymmetric models with minimal flavour violation and their running*, *Eur. Phys. J.* **C59** (2009) 75–98, [0807.0801].
- [9] S. Heinemeyer, X. Miao, S. Su, and G. Weiglein, *B-Physics Observables and Electroweak Precision Data in the CMSSM, mGMSB and mAMSB*, *JHEP* **08** (2008) 087, [0805.2359].
- [10] O. Buchmueller *et. al.*, *Prediction for the Lightest Higgs Boson Mass in the CMSSM using Indirect Experimental Constraints*, *Phys. Lett.* **B657** (2007) 87–94, [0707.3447].
- [11] H. P. Nilles, *Dynamically Broken Supergravity and the Hierarchy Problem*, *Phys. Lett.* **B115** (1982) 193.
- [12] A. H. Chamseddine, R. L. Arnowitt, and P. Nath, *Locally Supersymmetric Grand Unification*, *Phys. Rev. Lett.* **49** (1982) 970.
- [13] R. Barbieri, S. Ferrara, and C. A. Savoy, *Gauge Models with Spontaneously Broken Local Supersymmetry*, *Phys. Lett.* **B119** (1982) 343.
- [14] N. Ohta, *Grand unified theories based on local supersymmetry*, *Prog. Theor. Phys.* **70** (1983) 542.
- [15] L. J. Hall, J. D. Lykken, and S. Weinberg, *Supergravity as the Messenger of Supersymmetry Breaking*, *Phys. Rev.* **D27** (1983) 2359–2378.
- [16] S. K. Soni and H. A. Weldon, *Analysis of the Supersymmetry Breaking Induced by $N = 1$ Supergravity Theories*, *Phys. Lett.* **B126** (1983) 215.
- [17] H. Baer, M. Brhlik, D. Castano, and X. Tata, *$b \rightarrow s\gamma$ constraints on the minimal supergravity model with large $\tan \beta$* , *Phys. Rev.* **D58** (1998) 015007, [hep-ph/9712305].

- [18] B. Dudley and C. Kolda, *Supersymmetric Flavor-Changing Sum Rules as a Tool for $b \rightarrow s\gamma$* , *Phys. Rev.* **D79** (2009) 015011, [0805.4565].
- [19] J. R. Ellis, J. S. Lee, and A. Pilaftsis, *B-Meson Observables in the Maximally CP-Violating MSSM with Minimal Flavour Violation*, *Phys. Rev.* **D76** (2007) 115011, [0708.2079].
- [20] M. S. Carena, S. Mrenna, and C. E. M. Wagner, *MSSM Higgs boson phenomenology at the Tevatron collider*, *Phys. Rev.* **D60** (1999) 075010, [hep-ph/9808312].
- [21] M. Carena, D. Garcia, U. Nierste, and C. E. M. Wagner, *Effective Lagrangian for the $\bar{t}bH^+$ interaction in the MSSM and charged Higgs phenomenology*, *Nucl. Phys.* **B577** (2000) 88–120, [hep-ph/9912516].
- [22] C. Hamzaoui, M. Pospelov, and M. Toharia, *Higgs-mediated FCNC in supersymmetric models with large $\tan\beta$* , *Phys. Rev.* **D59** (1999) 095005, [hep-ph/9807350].
- [23] K. S. Babu and C. F. Kolda, *Higgs-mediated $B^0 \rightarrow \mu^+\mu^-$ in Minimal Supersymmetry*, *Phys. Rev. Lett.* **84** (2000) 228–231, [hep-ph/9909476].
- [24] A. Dedes, H. Dreiner, and U. Nierste, *Correlation of $B_s \rightarrow \mu^+\mu^-$ and $(g-2)_\mu$ in minimal supergravity*, *Phys. Rev. Lett.* **87** (2001) 251804, [hep-ph/].
- [25] T. Blazek, S. Raby, and S. Pokorski, *Finite supersymmetric threshold corrections to CKM matrix elements in the large $\tan\beta$ regime*, *Phys. Rev.* **D52** (1995) 4151–4158, [hep-ph/9504364].
- [26] A. Crivellin and U. Nierste, *Supersymmetric renormalisation of the CKM matrix and new constraints on the squark mass-matrices*, *Phys. Rev.* **D79** (2009) 035018, [0810.1613].
- [27] G. Isidori and P. Paradisi, *Hints of large $\tan\beta$ in flavour physics*, *Phys. Lett.* **B639** (2006) 499–507, [hep-ph/0605012].
- [28] U. Nierste, S. Trine, and S. Westhoff, *Charged-Higgs effects in a new $B \rightarrow D\tau\bar{\nu}$ differential decay distribution*, *Phys. Rev.* **D78** (2008) 015006, [0801.4938 [hep-ph]].
- [29] J. F. Kamenik and F. Mescia, *$B \rightarrow D\tau\bar{\nu}$ Branching Ratios: Opportunity for Lattice QCD and Hadron Colliders*, *Phys. Rev.* **D78** (2008) 014003, [0802.3790].
- [30] A. J. Buras, P. H. Chankowski, J. Rosiek, and L. Slawianowska, *$\Delta M_s/\Delta M_d$, $\sin 2\beta$ and the angle γ in the presence of new $\Delta F = 2$ operators*, *Nucl. Phys.* **B619** (2001) 434–466, [hep-ph/0107048].
- [31] T. A. *et al.* [CDF Collaboration], *Search for $B_s \rightarrow \mu^+\mu^-$ and $B_d \rightarrow \mu^+\mu^-$ decays with $2fb^{-1}$ of $p\bar{p}$ collisions*, *Phys. Rev. Lett.* **100** (2008) 101802, [0712.1708 [hep-ph]].
- [32] **D0** Collaboration, V. M. Abazov *et. al.*, *A search for the flavor-changing neutral current decay $B_s^0 \rightarrow \mu^+\mu^-$ in $p\bar{p}$ collisions at $\sqrt{s} = 1.96$ TeV with the DØ detector*, *Phys. Rev. Lett.* **94** (2005) 071802, [hep-ex/0410039].
- [33] A. J. Buras, P. H. Chankowski, J. Rosiek, and L. Slawianowska, *Correlation between ΔM_s and $B_{s,d}^0 \rightarrow \mu^+\mu^-$ in Supersymmetry at large $\tan\beta$* , *Phys. Lett.* **B546** (2002) 96–107, [hep-ph/0207241].

-
- [34] G. Isidori and A. Retico, *Scalar flavour-changing neutral currents in the large- $\tan\beta$ limit*, *JHEP* **11** (2001) 001, [hep-ph/0110121].
 - [35] A. J. Buras, P. H. Chankowski, J. Rosiek, and L. Slawianowska, $\Delta M_{d,s}$, $B_{d,s}^0 \rightarrow \mu^+ \mu^-$ and $B \rightarrow X_s \gamma$ in Supersymmetry at Large $\tan\beta$, *Nucl. Phys.* **B659** (2003) 3, [hep-ph/0210145].
 - [36] M. Gorbahn, S. Jäger, U. Nierste, and S. Trine, *The supersymmetric Higgs sector and $B - \bar{B}$ mixing for large $\tan\beta$* , *arXiv:0901.2065 [hep-ph]* (2009) [0901.2065].
 - [37] M. Beneke, P. Ruiz-Femenia, and M. Spinrath, *Higgs couplings in the MSSM at large $\tan\beta$* , *JHEP* **01** (2009) 031, [0810.3768].
 - [38] M. S. Carena, D. Garcia, U. Nierste, and C. E. M. Wagner, $b \rightarrow s \gamma$ and supersymmetry with large $\tan\beta$, *Phys. Lett.* **B499** (2001) 141–146, [hep-ph/0010003].
 - [39] G. Degrandi, P. Gambino, and G. F. Giudice, $B \rightarrow X_s \gamma$ in supersymmetry: Large contributions beyond the leading order, *JHEP* **12** (2000) 009, [hep-ph/0009337].
 - [40] J. Guasch, R. Jimenez, and J. Sola, *Supersymmetric QCD corrections to the charged Higgs boson decay of the top quark*, *Phys. Lett.* **B360** (1995) 47, [hep-ph/9507461].
 - [41] C. S. Huang, W. Liao, Q. S. Yan, and S. H. Zhu, $B_s \rightarrow \ell^+ \ell^-$ in a general 2HDM and MSSM, *Phys. Rev.* **D63** (2001) 114021 [Erratum-ibid. **D64** (2001) 059902], [hep-ph/0006250].
 - [42] S. Marchetti, S. Mertens, U. Nierste, and D. Stöckinger, $\tan\beta$ -enhanced supersymmetric corrections to the anomalous magnetic moment of the muon, *Phys. Rev.* **D79** (2009) 013010, [0808.1530].
 - [43] P. Skands *et. al.*, *SUSY Les Houches accord: Interfacing SUSY spectrum calculators, decay packages, and event generators*, *JHEP* **07** (2004) 036, [hep-ph/0311123].
 - [44] D. M. Pierce, J. A. Bagger, K. T. Matchev, and R.-J. Zhang, *Precision corrections in the minimal supersymmetric standard model*, *Nucl. Phys.* **B491** (1997) 3–67, [hep-ph/9606211].
 - [45] G. Gamberini, G. Ridolfi, and F. Zwirner, *On Radiative Gauge Symmetry Breaking in the Minimal Supersymmetric Model*, *Nucl. Phys.* **B331** (1990) 331–349.
 - [46] Y. Yamada, *Two-loop renormalization of $\tan\beta$ and its gauge dependence*, *Phys. Lett.* **B530** (2002) 174–178, [hep-ph/0112251].
 - [47] A. Freitas and D. Stöckinger, *Gauge dependence and renormalization of $\tan\beta$ in the MSSM*, *Phys. Rev.* **D66** (2002) 095014, [hep-ph/0205281].
 - [48] H. E. Logan and U. Nierste, $B_{s,d} \rightarrow \ell^+ \ell^-$ in a two-Higgs-doublet model, *Nucl. Phys.* **B586** (2000) 39–55, [hep-ph/0004139].
 - [49] J. Küblbeck, M. Bohm, and A. Denner, *FeynArts: Computer Algebraic Generation of Feynman Graphs and Amplitudes*, *Comput. Phys. Commun.* **60** (1990) 165–180.
 - [50] T. Hahn, *Generating Feynman diagrams and amplitudes with FeynArts 3*, *Comput. Phys. Commun.* **140** (2001) 418–431, [hep-ph/0012260].

- [51] G. Degrandi, P. Gambino, and P. Slavich, *QCD corrections to radiative B decays in the MSSM with minimal flavor violation*, *Phys. Lett.* **B635** (2006) 335–342, [hep-ph/0601135].
- [52] A. Denner and T. Sack, *Renormalization of the quark mixing matrix*, *Nucl. Phys.* **B347** (1990) 203–216.
- [53] P. Gambino, P. A. Grassi, and F. Madricardo, *Fermion mixing renormalization and gauge invariance*, *Phys. Lett.* **B454** (1999) 98–104, [hep-ph/9811470].
- [54] J. A. Casas, A. Lleyda, and C. Munoz, *Strong constraints on the parameter space of the MSSM from charge and color breaking minima*, *Nucl. Phys.* **B471** (1996) 3–58, [hep-ph/9507294].
- [55] J. A. Casas and S. Dimopoulos, *Stability bounds on flavor-violating trilinear soft terms in the MSSM*, *Phys. Lett.* **B387** (1996) 107–112, [hep-ph/9606237].
- [56] S. Pokorski, J. Rosiek, and C. A. Savoy, *Constraints on phases of supersymmetric flavour conserving couplings*, *Nucl. Phys.* **B570** (2000) 81–116, [hep-ph/9906206].
- [57] M. Beneke, X.-Q. Li, and L. Vernazza, *Hadronic B decays in the MSSM with large $\tan \beta$* , *Eur. Phys. J.* **C61** (2009) 429–438, [0901.4841].
- [58] D. A. Demir and K. A. Olive, *$B \rightarrow X_s \gamma$ in supersymmetry with explicit CP violation*, *Phys. Rev.* **D65** (2002) 034007, [hep-ph/0107329].
- [59] M. E. Gomez, T. Ibrahim, P. Nath, and S. Skadhauge, *An improved analysis of $b \rightarrow s \gamma$ in Supersymmetry*, *Phys. Rev.* **D74** (2006) 015015, [hep-ph/0601163].
- [60] C. Bobeth, A. J. Buras, and T. Ewerth, *$\bar{B} \rightarrow X_s \ell^+ \ell^-$ in the MSSM at NNLO*, *Nucl. Phys.* **B713** (2005) 522–554, [hep-ph/0409293].
- [61] A. Dedes, J. Rosiek, and P. Tanedo, *Complete One-Loop MSSM Predictions for $B^0 \rightarrow \ell^+ \ell'^-$ at the Tevatron and LHC*, *Phys. Rev.* **D79** (2009) 055006, [0812.4320].
- [62] A. L. Kagan and M. Neubert, *QCD anatomy of $B \rightarrow X_s \gamma$ decays*, *Eur. Phys. J.* **C7** (1999) 5–27, [hep-ph/9805303].
- [63] M. Ciuchini, G. Degrandi, P. Gambino, and G. F. Giudice, *Next-to-leading QCD corrections to $B \rightarrow X_s \gamma$ in supersymmetry*, *Nucl. Phys.* **B534** (1998) 3–20, [hep-ph/9806308].
- [64] M. Beneke, G. Buchalla, M. Neubert, and C. T. Sachrajda, *QCD factorization for exclusive, non-leptonic B meson decays: General arguments and the case of heavy-light final states*, *Nucl. Phys.* **B591** (2000) 313–418, [hep-ph/0006124].
- [65] M. Beneke and M. Neubert, *QCD factorization for $B \rightarrow PP$ and $B \rightarrow PV$ decays*, *Nucl. Phys.* **B675** (2003) 333–415, [hep-ph/0308039].
- [66] G. Buchalla, G. Hiller, Y. Nir, and G. Raz, *The pattern of CP asymmetries in $b \rightarrow s$ transitions*, *JHEP* **09** (2005) 074, [hep-ph/0503151].
- [67] W. Altmannshofer, A. J. Buras, and P. Paradisi, *Low Energy Probes of CP Violation in a Flavor Blind MSSM*, *Phys. Lett.* **B669** (2008) 239–245, [0808.0707].
- [68] A. Dedes and A. Pilaftsis, *Resummed effective Lagrangian for Higgs-mediated FCNC interactions in the CP -violating MSSM*, *Phys. Rev.* **D67** (2003) 015012, [hep-ph/0209306].

- [69] J. R. Ellis, S. Heinemeyer, K. A. Olive, and G. Weiglein, *Light Heavy MSSM Higgs Bosons at Large $\tan \beta$* , *Phys. Lett.* **B653** (2007) 292–299, [0706.0977].
- [70] S. Heinemeyer, W. Hollik, H. Rzehak, and G. Weiglein, *High-precision predictions for the MSSM Higgs sector at $\mathcal{O}(\alpha_b)$ and $\mathcal{O}(\alpha_s)$* , *Eur. Phys. J.* **C39** (2005) 465–481, [hep-ph/0411114].